Specifically differentiated T cell subset promotes tumor immunity over fatal immunity

Abdulraouf Ramadan,[1] Brad Griesenauer,[1] Djamilatou Adom,[1] Reuben Kapur,[1] Helmut Hanenberg,[1] Chen Liu,[2] Mark H. Kaplan,[1] and Sophie Paczesny[1]

[1]Indiana University School of Medicine, Indianapolis, IN
[2]Rutgers Robert Wood Johnson Medical School, New Brunswick, NJ

Allogeneic immune cells, particularly T cells in donor grafts, recognize and eliminate leukemic cells via graft-versus-leukemia (GVL) reactivity, and transfer of these cells is often used for high-risk hematological malignancies, including acute myeloid leukemia. Unfortunately, these cells also attack host normal tissues through the often fatal graft-versus-host disease (GVHD). Full separation of GVL activity from GVHD has yet to be achieved. Here, we show that, in mice and humans, a population of interleukin-9 (IL-9)–producing T cells activated via the ST2–IL-33 pathway ($T9_{IL-33}$ cells) increases GVL while decreasing GVHD through two opposing mechanisms: protection from fatal immunity by amphiregulin expression and augmentation of antileukemic activity compared with T9, T1, and unmanipulated T cells through CD8α expression. Thus, adoptive transfer of allogeneic $T9_{IL-33}$ cells offers an attractive approach for separating GVL activity from GVHD.

INTRODUCTION

One of the most validated immunotherapies to date, allogeneic hematopoietic cell transplantation (HCT), is a potentially curative option for high-risk hematological malignancies, including acute myeloid leukemia (AML), which affected >20,000 patients and led to >10,000 deaths in the United States alone in 2015 (American Cancer Society, 2015) and thus constitutes a critical unmet therapeutic need. Graft-versus-leukemia (GVL) reactivity requires donor T cell recognition of alloantigens on tumor cells (van den Brink and Burakoff, 2002; Warren and Deeg, 2013; Othus et al., 2015). Allogeneic-specific T cells can be generated without gene transfer and exhibit adequate T cell receptor affinity (Bachireddy et al., 2015; Cruz and Bollard, 2015; Dotti, 2015). Unfortunately, their reactivity to alloantigens in normal host tissues often leads to graft-versus-host disease (GVHD), a major cause of death after HCT. We previously showed that elevated plasma soluble stimulation 2 (sST2) is a risk factor of therapy-resistant GVHD and death (Vander Lugt et al., 2013). ST2 blockade reduces sST2-producing T cells while maintaining membrane ST2 (mST2)–expressing T helper type 2 (Th2) and mST2 FoxP3$^+$ regulatory T ($ST2^+$ T reg) cells during GVHD (Zhang et al., 2015). Adoptive cell transfer (ACT) of in vitro differentiated total T2 cells (T cells containing CD4$^+$ and CD8$^+$ T cells differentiated under type 2 conditions [IL-4]) did not induce GVHD as severely as T1 cells (T cells containing CD4$^+$ and CD8$^+$ T cells differentiated under type 1 conditions [IL-12]); however, T2 cells did not show any antileukemic activity (Jung et al., 2003; Tawara et al., 2008). Thought to be associated with Th2 responses and arising from reprogrammed Th2 cells upon stimulation with TGF-β (Dardalhon et al., 2008; Veldhoen et al., 2008), Th9 cells (T cells containing only CD4$^+$ cells differentiated under type 9 conditions [IL-4 + TGF-β]) were originally shown to be a subset of CD4 T cells that differed from Th2 cells in that Th9 cells produce IL-9 and little IL-4 and express the ETS transcription factor PU.1 (Chang et al., 2005, 2010). It has been shown that Th2 cells express mST2 (Löhning et al., 1998; Xu et al., 1998), and the addition of IL-33 with TGF-β further increased mST2 expression on these cells (Blom et al., 2011). Reducing circulating sST2 driven by type 1 immune response with a neutralizing antibody led to protection against GVHD (Zhang et al., 2015) and increased mST2 expression on T reg cells, suggesting that ACT of mST2 expressing T cells represents a potential novel therapeutic approach to protect against GVHD. Thus, we were interested in IL-9–producing T cells because (a) ACT of these cells may protect against GVHD, similar to T2 cells or regulatory T cells; (b) IL-9 neutralization decreased the antitumor activity of T cells in melanoma models (Purwar et al., 2012); and (c) Th9 cells and IL-9–producing cytotoxic CD8 (Tc9) cells showed higher antitumor activity than Th1 and Tc1 cells in the same melanoma models (Lu et al., 2012, 2014). Whether or not Th9 and Tc9 (together T9 cells) express mST2, like T2, and how this ST2–IL-33 signaling affects T9 cells is unknown. In this study, we hypothesized that (a) the activation of T9 cells with

Correspondence to Sophie Paczesny: sophpacz@iu.edu

Abbreviations used: ACT, adoptive cell transfer; AML, acute myeloid leukemia; AREG, amphiregulin; BM, bone marrow; EGFR, epidermal growth factor receptor; GVHD, graft-versus-host disease; GVL, graft versus leukemia; Gzm, granzyme; HCT, hematopoietic cell transplantation; ILC2, type 2 innate lymphoid cell; MLL-AF9, mixed-lineage leukemia and AF9 fusion protein; MLR, mixed lymphocyte reaction; mST2, membrane ST2; Prf, perforin; sST2, soluble ST2; TCD, T cell depleted.

The Rockefeller University Press
J. Exp. Med. 2017 Vol. 214 No. 12 3577–3596
https://doi.org/10.1084/jem.20170041

IL-33 during differentiation will enhance mST2 and IL-9 expression and (b) ACT of IL-33 activated T9 cells ($T9_{IL-33}$) will decrease GVHD severity and possibly increase GVL activity.

RESULTS

ST2–IL-33 signaling increases mST2, IL-9, and PU.1 expression on T9 cells

To investigate the impact of ST2–IL-33 signaling on T9 differentiation, we polarized total T cells from C57BL/6 mice into T9 cells in the presence ($T9_{IL-33}$) or absence (T9) of IL-33. T9 cells expressed mST2 at the protein level, and mST2 protein expression on $T9_{IL-33}$ cells was further increased on both CD4 and CD8 T cells (Fig. 1 A). PU.1 expression, a master transcription factor that promotes IL-9 production, was up-regulated in both CD4 and CD8 T cells upon addition of IL-33 during T9 differentiation. $T9_{IL-33}$ cells have increased IL-9 expression in CD4 (>70% of total CD4 T cells expressing IL-9) and CD8 (>50% of total CD8 T cells expressing IL-9). IL-9 secretion from these cells was also increased. $T9_{IL-33}$ cells did not secrete IFN-γ, IL-4, or sST2 in comparison with other differentiated T cell subsets (T1 and T2; Fig. 1 C; and Fig. S1, A and B). However, no expansion of T reg cells occurred during murine $T9_{IL-33}$ differentiation in vitro (Fig. S1 C). Human T9 cells are poorly characterized. Our results demonstrate that, like murine $T9_{IL-33}$ cells, differentiation of human T9 cells in the presence of IL-33 enhanced mST2 and PU.1 expressions as well as IL-9 expression and secretion by CD4 and CD8 T cells compared with other T cell subsets, including T9 cells (Fig. 1, D–F; and Fig. S1 D).

ACT of $T9_{IL-33}$ cells reduces GVHD severity

We next evaluated the in vivo function of allogeneic $T9_{IL-33}$ cells in comparison with freshly isolated unmanipulated T cells and T0 (without polarizing cytokines), T1, T2, T9, and $T9_{IL-33}$ cells in a major histocompatibility antigen mismatch model of HCT. Mice receiving unmanipulated T, T0, or T1 cells showed severe GVHD and high mortality, whereas mice receiving T2 or T9 cells showed moderate GVHD with 40–60% survival. GVHD was almost completely abrogated in animals receiving $T9_{IL-33}$ cells, with 100% survival in these mice (Fig. 1 G). Compared with the WT $T9_{IL-33}$ group, ACT of $T9_{IL-33}$ cells generated from $ST2^{-/-}$ or $IL\text{-}9^{-/-}$ T cells resulted in significantly more severe GVHD and reduced survival (Fig. 1 H). The role of the ST2–IL-33 axis was confirmed in a minor histocompatibility antigen model of GVHD (Fig. 1 I).

Pathological examination of the intestines during GVHD showed less tissue damage in mice that received $T9_{IL-33}$ cells versus T1 cells (Fig. 2 A). To understand the mechanism responsible for the protective effect by $T9_{IL-33}$ cells against lower intestinal epithelium damage during GVHD, we explored several possibilities. First, ex vivo analysis of T cells in the gut, the major GVHD target organ, 10 d after transplantation showed no difference in T cell proliferation between groups, as measured by carboxyfluorescein succinimidyl ester (CFSE) staining (Fig. 2 B), or the total number of gut-infiltrating T cells (Fig. 2 C). Second, we avoided possible differences in apoptosis and migration capacities (Waldman et al., 2006; Reshef et al., 2012; Huang et al., 2015) between WT $T9_{IL-33}$ and $ST2^{-/-}$ $T9_{IL-33}$ cells in the intestine by measuring Annexin-V, α4β7, CRK (v-crk sarcoma virus CT10 oncogene homologue [avian], also called p38; Huang et al., 2015), and CCR5 expression (Fig. 2, D and E). Third, although $ST2^{+}$ T reg cells and type 2 innate lymphoid cells (ILC2s) reduce GVHD severity (Munneke et al., 2014; Zhang et al., 2015), no difference in T reg frequency was observed after transfer of WT $T9_{IL-33}$, T1, or $ST2^{-/-}$ $T9_{IL-33}$ cells, and ILC2 cells were absent in the intestine of all HCT groups (Fig. 2, F and G). To confirm that the GVHD protective phenotype was not due to contaminating T reg cells in the graft and/or following homeostatic proliferation, we used the Foxp3-GFP reporter to differentiate total T cells toward $T9_{IL-33}$ cells and then adoptively transferred either non–Foxp3-GFP–depleted $T9_{IL-33}$ cells or Foxp3-GFP–depleted $T9_{IL-33}$ cells (by cell sorting) to remove any Foxp3 T reg cells from the graft. We did not notice any expansion of Foxp3-GFP^{+} T reg cells ex vivo in the gut at day 14 or any differences in clinical scores for GVHD or in survival rates between the two groups (Fig. 2, H and I). These data indicate that ST2–IL-33 and IL-9 signaling are critical for $T9_{IL-33}$ cell–mediated protection against GVHD, independent of T reg cells, and that this protection is not due to differences in proliferation, apoptosis, or migration of the $T9_{IL-33}$ cells compared with other T cell subsets. As well, Foxp3-GFP depletion does not impact GVHD protection in mice that received $T9_{IL-33}$ cells.

IL-33 induces amphiregulin (AREG) expression on T9 cells alleviating GVHD

We then used Transwell assays of T cells with allogeneic colonic epithelial cells and showed that WT $T9_{IL-33}$ cells were able to maintain live colonic cells almost at the level of the control co-culture without T cells, whereas T1 and $ST2^{-/-}$ $T9_{IL-33}$ cells (equivalent to T9 cells) killed ∼70% and ∼40% of the allogeneic colonic cells, respectively, in a contact-dependent manner (no differences in Transwell assays; Fig. 3 A). Next, we analyzed AREG, because its expression on mST2-expressing cells is involved in tissue repair via the ST2–IL-33 axis independent of TCR signaling (Zaiss et al., 2013; Arpaia et al., 2015; Monticelli et al., 2015). AREG has not previously been explored on T cell subsets other than T reg cells. We compared the expression of AREG on different in vitro differentiated T cell subsets (T1, T2, T9, WT $T9_{IL-33}$, $ST2^{-/-}$ $T9_{IL-33}$, and T reg cells) and found that WT $T9_{IL-33}$ cells expressed as much AREG as T reg cells and that the expression of AREG on $T9_{IL-33}$ cells was independent of Foxp3 expression (Fig. 3, B and C). Blocking AREG in co-cultured epithelial cells and allogeneic WT $T9_{IL-33}$ cells decreased epithelial cell viability at rates comparable to those observed with T1, T9, or $ST2^{-/-}$ $T9_{IL-33}$ cells (Fig. 3, D and E). As T reg cells can suppress the function of other T cell subsets (Fontenot et al., 2003), we next tested whether $T9_{IL-33}$ cells could

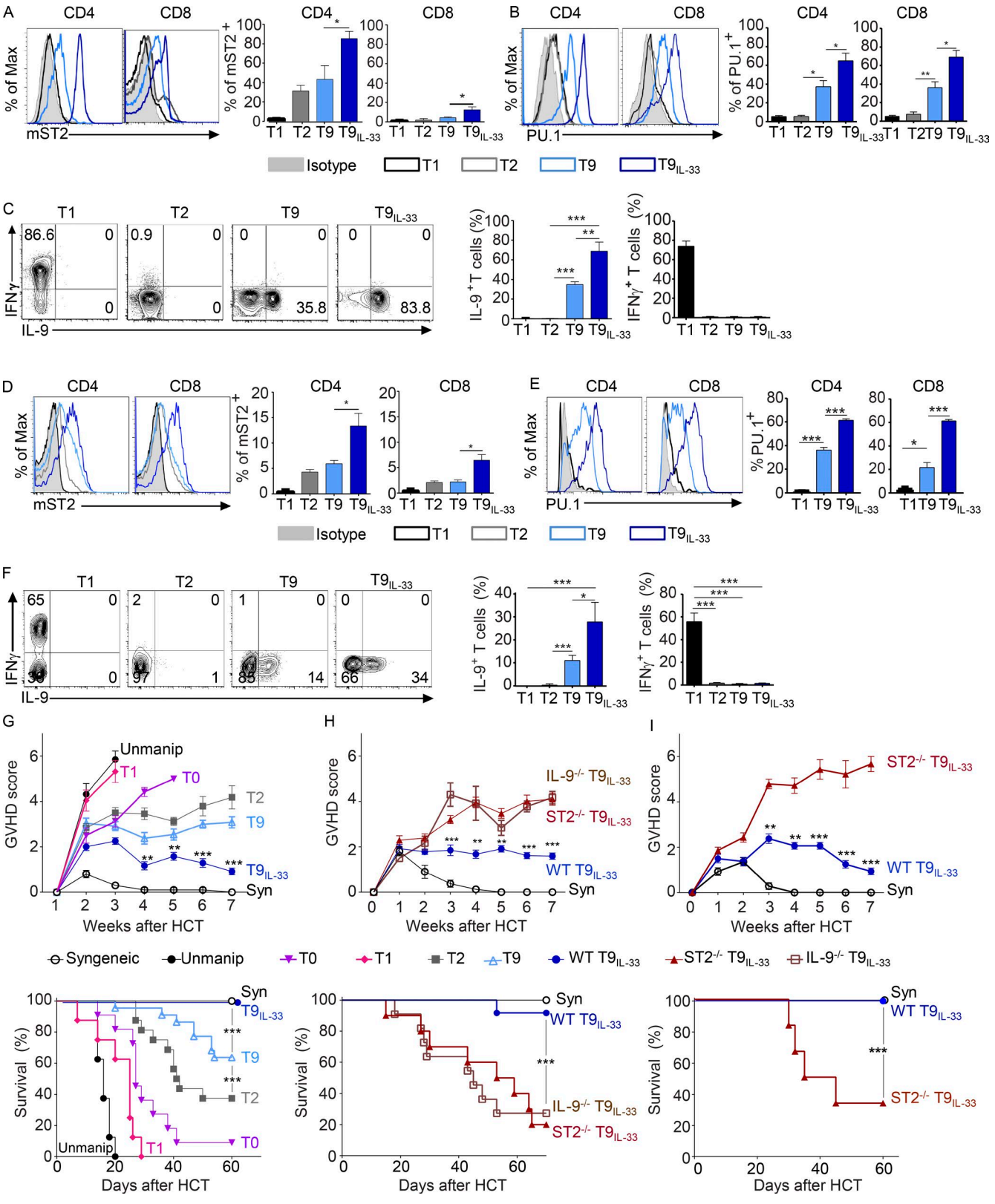

Figure 1. **IL-33 enhances mST2, IL-9, and PU.1 expression on T9 cells, and adoptive transfer of $T9_{IL-33}$ cells improves GVHD and survival after allo-HCT.** (A) Representative histogram of mST2 expression on murine CD4 and CD8 T cell subsets after 5 d of differentiation ($n = 5$, from five independent experiments, unpaired t test; data are shown as mean ± SEM; *, $P < 0.05$). (B) Representative histogram of mouse PU.1 expression in CD4 and CD8 T cell

be T cell suppressive–like T reg cells. We found that $T9_{IL\text{-}33}$ cells could not suppress the function of T1 cells (Fig. 3 F). In addition, we did not observe a difference in the suppressive abilities of T reg cells with AREG blockade (Fig. 3 F), as previously shown by Arpaia et al. (2015) with genetic ablation of AREG. Thus, $T9_{IL\text{-}33}$ cells do not behave like T reg cells, and they do not show a suppressive function toward other types of T cells. Ex vivo analysis of sorted T cells from intestine of HCT models also showed that AREG expression was greater in WT $T9_{IL\text{-}33}$ cells than in T1 or $ST2^{-/-}$ $T9_{IL\text{-}33}$ cells (Fig. 3 G). Furthermore, AREG blockade in HCT recipients receiving $T9_{IL\text{-}33}$ increased the severity of GVHD and mortality in comparison with mice treated with isotype control (Fig. 3 H). AREG blockade did not change IFN-γ expression by gut-infiltrating T cells at day 10 after HCT (Fig. 3 I). These data are consistent with the in vitro data showing that $T9_{IL\text{-}33}$ cells do not have a direct immunosuppressive effect with other T cells (Fig. S3 C). AREG expression by ex vivo isolated gut T cells at day 10 after HCT was not changed in mice receiving Foxp3-GFP–depleted or nondepleted $T9_{IL\text{-}33}$ cells (Fig. 3 J). Plasma levels of sST2, TNF, and IFN-γ (Fig. 4, A and B) were lower in mice receiving $T9_{IL\text{-}33}$ than in mice receiving T1 or T9 cells, suggesting a counterbalance of the excess of systemic sST2 generated during GVHD by mST2 on $T9_{IL\text{-}33}$ cells. The increase in AREG (Fig. 3 B) is also dependent on IL-9 expression, as $IL\text{-}9^{-/-}$ $T9_{IL\text{-}33}$ cells expressed very low levels of AREG compared with WT $T9_{IL\text{-}33}$ cells (Fig. 4 C). The increased mST2 and decreased sST2 expression observed (Figs. 1 A and 2 I) was also dependent on IL-9 (Fig. 4 D). Although AREG blockade did not change the frequencies of IFN-γ– or IL-17–producing T cells, we observed overall a lower frequency of pathogenic cells producing IFN-γ and IL-17 in the gut at day 10 after HCT (Fig. 4 E). The levels of IFN-γ and IL-17 expression in T cells from the gut at day 10 after allo-HCT were also similar in C3H.SW mice receiving either allogeneic Foxp3-GFP–depleted or Foxp3-GFP–nondepleted $T9_{IL\text{-}33}$ cells (Fig. 4 F). Human $T9_{IL\text{-}33}$ cells also exhibited higher AREG expression than T1 cells (that do express ∼1%) and T9 cells (∼4%, significantly lower than ∼15% in $T9_{IL\text{-}33}$ cells; Fig. 4 G). AREG blockade during co-culture with human allogeneic colonic epithelial cells decreased the protective effect of human $T9_{IL\text{-}33}$ to levels seen with T9 cells (Fig. 4 H). Together, our data suggest that activation of the ST2–IL-33 pathway up-regulates AREG expression on both murine and human $T9_{IL\text{-}33}$ cells and provides protection against epithelial damage during alloreaction, leading to a low degree of GVHD after ACT of $T9_{IL\text{-}33}$ cells.

$T9_{IL\text{-}33}$ cells exhibit better antileukemic activity than T1 cells

We next investigated whether ACT of $T9_{IL\text{-}33}$ cells maintained antitumor activity. In recipients with lymphoma (A20), compared with syngeneic or allogeneic T cell subsets (unmanipulated T, T1, and T9), transfer of WT $T9_{IL\text{-}33}$ cells resulted in milder GVHD without impairing antitumor activity, as more than 85% of these mice survived past 80 d after HCT and were GVHD/tumor free. In contrast, mice receiving unmanipulated T or T1 cells all died early of GVHD. In mice receiving T9 or $ST2^{-/-}$ $T9_{IL\text{-}33}$ cells, GVHD onset was delayed and 60% died of tumor by day 60 (Fig. 5 A). The same trends were observed in recipients with mixed-lineage leukemia and AF9 fusion protein (MLL-AF9) AML in both major MHC and minor histocompatibility antigen HCT models (Fig. 5, B and C). Most mice receiving $IL\text{-}9^{-/-}$ $T9_{IL\text{-}33}$ cells died of leukemia (Fig. 5 B). We then compared the transcriptomes of WT $T9_{IL\text{-}33}$ versus $ST2^{-/-}$ $T9_{IL\text{-}33}$ cells in CD8 and CD4 sorted populations and found higher expression of cytolytic molecules (granzyme a [Gzma], Gzmb, perforin [Prf1], and Fas) as well as markers of the T cell central memory phenotype (Cd62l and Cd27; Fig. 5 D, Fig. S2, and Table S2), which have been shown to correlate with higher antitumor activity (Klebanoff et al., 2016). Expression of cytolytic molecules was confirmed at the protein level (Fig. 5 E). Furthermore, ex vivo bone marrow (BM)–infiltrating CD8 T cells from $T9_{IL\text{-}33}$ recipients expressed more Gzmb and Prf1 (Fig. 5 F). Total WT $T9_{IL\text{-}33}$ cells showed more lysis against MLL-AF9 AML than total allogeneic T cells derived from unmanipulated T, T1, T9, $ST2^{-/-}$ $T9_{IL\text{-}33}$, or syngeneic $T9_{IL\text{-}33}$ cells (Fig. 6 A). Both sorted CD4 and CD8 cells from total allogeneic WT $T9_{IL\text{-}33}$ cells showed higher antitumor activity (∼60% and 80% at a T/target ratio of 10:1, respectively) than CD4 and

subsets after 5 d of differentiation (n = 5, from five independent experiments, unpaired t test; data are shown as mean ± SEM; *, P < 0.05; **, P < 0.01). (C) Representative plots of IL-9 and IFN-γ expression from in vitro differentiated murine cells and a bar graphs showing the frequency of IL-9– and IFN-γ expressing T cells (n = 4, from four independent experiments, unpaired t test; data are shown as mean ± SEM; *, P < 0.05; **, P < 0.01; ***, P < 0.001). (D) mST2 expression on human CD4 and CD8 T cell subsets after 7 d of differentiation (n = 4, from four independent experiments, unpaired t test; data are shown as mean ± SEM; *, P < 0.05, mean ± SEM). (E) Representative histogram of PU.1 expression in human CD4 and CD8 T cell subsets after 7 d of differentiation (n = 3, from three independent experiments unpaired t test; data are shown as mean ± SEM; *, P < 0.05; ***, P < 0.001). (F) Representative plots of IL-9 and IFN-γ expression in human T cells differentiated into T9 cells in the presence or absence of IL-33, and bar graphs showing the frequency of IL-9– and IFN-γ–expressing T cells (n = 4, from four independent experiments, unpaired t test; data are shown as mean ± SEM; *, P < 0.05; ***, P < 0.001). (G) Clinical scores of GVHD and survival curves for BALB/c mice transplanted with B6 or syngeneic BM cells and in vitro differentiated or freshly isolated syngeneic T cells (n = 12 each group, from two independent experiments unpaired t test; data are shown as mean ± SEM; ***, P < 0.001). (H) Clinical scores of GVHD and survival curves for BALB/c mice receiving B6 or syngeneic BM cells and in vitro differentiated or freshly isolated syngeneic T cells (n = 24 per group, from three independent experiments, unpaired t test; data are shown as mean ± SEM; **, P < 0.01; ***, P < 0.001). (I) Clinical scores of GVHD and survival curves for C3H.SW mice receiving B6 or syngeneic BM cells and in vitro differentiated or freshly isolated syngeneic T cells (n = 7 per group, unpaired t test; data are shown as mean ± SEM; **, P < 0.01; ***, P < 0.001). For survival by log-rank test; **, P < 0.01; ***, P < 0.001.

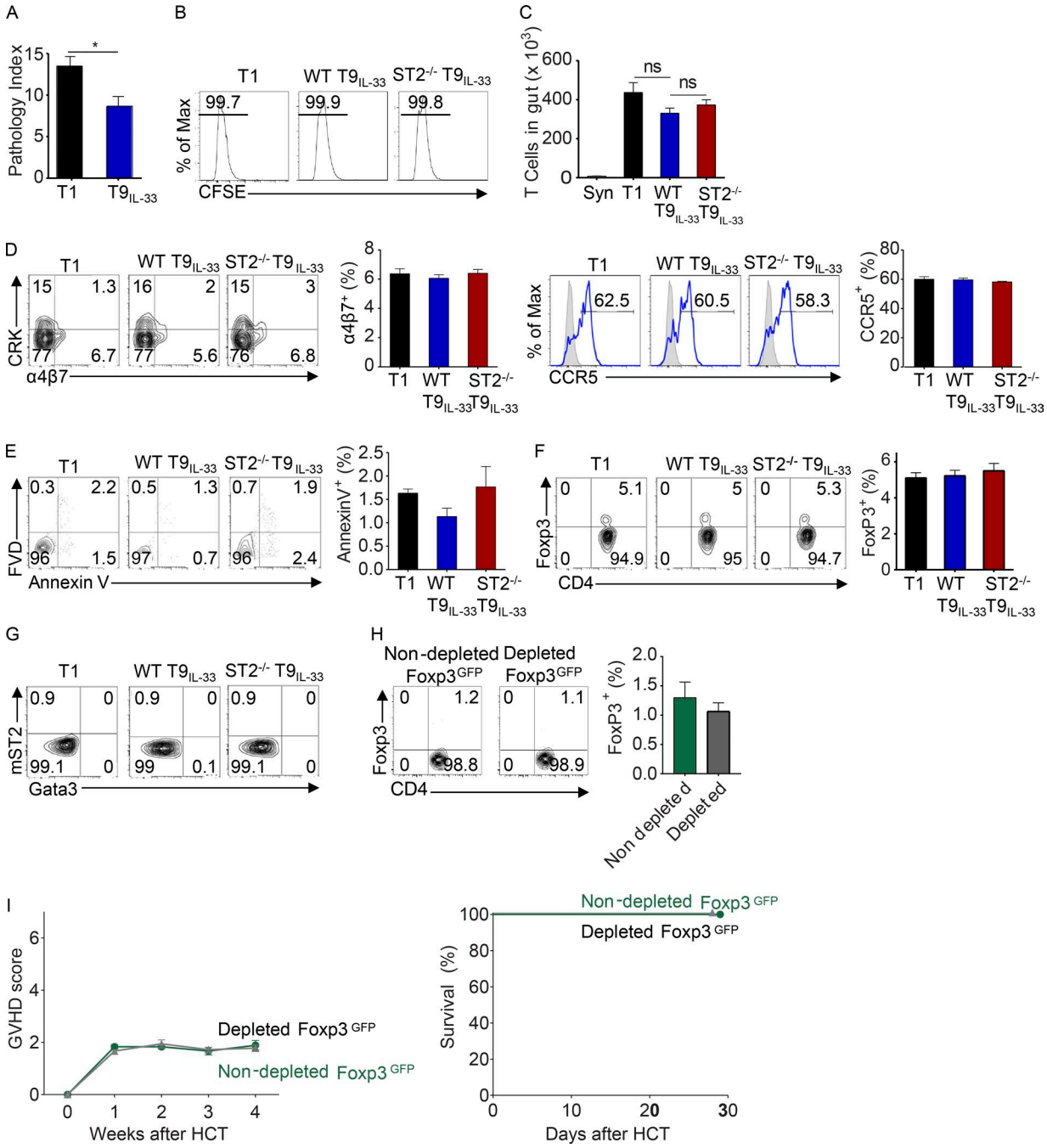

Figure 2. **Impact of T1 versus $T9_{IL-33}$ cells on gut pathology and effect of ST2–IL-33 signaling on gut T cell proliferation, viability, and migration, T reg expansion, and ILC2 expansion.** (A) Pathology index of mouse intestines at day 10 after allo-HCT with either T1 or $T9_{IL-33}$ cells ($n = 3$, from three independent experiments, unpaired *t* test; data are shown as mean ± SEM; *, $P < 0.05$). Specimens were harvested, placed in 10% buffered formalin, embedded in paraffin, cut into 5-µm-thick sections, and stained with hematoxylin and eosin for histological examination. Slides were coded without reference to mouse type or prior treatment status and examined systematically by a single pathologist. (B) Representative plots of CFSE-labeled in gut T cells collected from mice on day 5 after all-HCT with syngeneic BALB/c T cells or allogeneic in vitro differentiated T cells. (C) Absolute counts of gut-infiltrating T cells from mice on day 10 after allo-HCT with syngeneic BALB/c T cells or allogeneic in vitro differentiated T cells ($n = 3$, mean ± SEM, from three independent experiments, unpaired *t* test; data are shown as mean ± SEM). (D) Representative plots of α4β7 and CRK (v-crk sarcoma virus CT10 oncogene homologue [avian], also called p38) and CCR5 in CD4 T cells infiltrating the gut at day 10 after HTC ($n = 3$, unpaired *t* test; data are shown as mean ± SEM). (E) Representative plots of Annexin V and fixable viability dye (FVD) staining of gut T cells at day 10 post-HTC ($n = 3$). (F) Representative plots of CD4 and FoxP3 and a bar graph showing the frequency of T reg cells ($CD4^+FoxP3^+$) in gut-infiltrating CD4 T cells at day 10 after HTC ($n = 4$, unpaired *t* test; data are shown as mean ± SEM). (G) Representative plots of mST2 and Gata3 in $Lin^-CD45^+CD90.2^+$ cells (ILC2 markers, $n = 4$, unpaired *t* test; data are shown as mean ± SEM). (H) Ex

CD8 sorted cells from ST2$^{-/-}$ T9$_{IL-33}$ cells (~20% and 55% at a T/target ratio of 10:1, respectively; Fig. 6 B). This antitumor effect was also dependent on IL-9, as IL-9$^{-/-}$ T9$_{IL-33}$ T cells had lower cytolytic activity than WT T9$_{IL-33}$ cells both in vivo (Fig. 5 B) and in vitro (Fig. 6 C). Importantly, AML cells do not express epidermal growth factor receptor (EGFR) and blocking AREG did not affect the killing of leukemic cells by T9$_{IL-33}$ cells, explaining AREG specificity for epithelial cells (Fig. 6 D). Compared with T9 and T1 cells, human T9$_{IL-33}$ cells exhibited enhanced production of Gzmb and Prf1 (Fig. 6 E) and enhanced cytolytic activity against MOLM14, an aggressive AML cell line with FLT3-ITD (fms-related tyrosine kinase 3 internal tandem duplication; Fig. 6 F). T9$_{IL-33}$ cells have a central memory phenotype (CD62L^{+}CD44^{+}CD27^{+}KLRG1^{low}) in vitro and ex vivo (Fig. 7, A and B) that is mediated through ST2–IL-33 signaling. In addition, short-term effector cells, defined as KLRG1^{+}CD27^{-} (Joshi et al., 2007), from CD8 WT T9$_{IL-33}$ cells expressed more Gzmb than CD8 ST2$^{-/-}$ T9$_{IL-33}$ cells in vitro (Fig. 7 C). Human T9$_{IL-33}$ cells also displayed enhanced central memory phenotypes (CD45RA^{-}CCR7^{+}; Sallusto et al., 1999) and (CD27^{+}KLRG1^{low}; Koch et al., 2008) compared with T1 and T9 cells (Fig. 7, D and E). Contact-dependent ST2–IL-33 signaling in CD4 T cells license CD8 T cells to express higher IL-9, PU.1, Gzmb, and Prf1 (Fig. 8, A and B) and a central memory phenotype (Fig. 8 C). As a result, CD8 differentiated toward Tc9$_{IL-33}$ without CD4 T cells exhibited lower killing than Tc9$_{IL-33}$ cells in the presence of CD4 (Fig. 8 D). We demonstrated that activation of the ST2–IL-33 pathway enhances antitumor activity through up-regulation of cytolytic molecules and maintains a central memory phenotype, as well as short-term effector cells, leading to improvements in antitumoral activity in vitro and in vivo.

IL-33 enhances CD8α expression in both mouse and human T9$_{IL-33}$ cells for better killing of leukemia

We next investigated the possible antitumoral activity mechanism of action through transcriptome analysis showing significant up-regulation of CD8α expression that was confirmed at the mRNA and protein levels on both CD4 and CD8 cells from WT T9$_{IL-33}$ cells compared with T1, T9, and ST2$^{-/-}$ T9$_{IL-33}$ cells (Table S2; and Fig. 9, A and B). Blocking CD8α during total T9$_{IL-33}$ cell (containing both CD4^{+} and CD8^{+} T cells) differentiation reduced their Gzmb expression and cytolytic activity against MLL-AF9 leukemic cells (Fig. 9, C and D). Blocking CD8α during cytolytic assays almost completely abolished the cytolytic activity of T9$_{IL-33}$ cells (Fig. 9 E). The requirement of CD8α contact for leukemia cell killing was confirmed by imaging studies in which T9$_{IL-33}$ cells coincubated with allogeneic MLL-AF9 leukemic cells showed SYTOX release (high-affinity nucleic acid stain that penetrates cells with compromised plasma membranes), whereas syngeneic T9$_{IL-33}$ cells or CD8α neutralized allogeneic T9$_{IL-33}$ cells did not (Fig. 9 F). Of note, blocking CD8α also led to decreased antitumor activity by T1 and T9$_{IL-33}$ cells. T9$_{IL-33}$ cells actually showed significantly lower antitumor activity than T1 cells ($P = 0.03$ at a T/target ratio of 10:1; Fig. 9 G). As shown in Fig. 5 B, WT T9$_{IL-33}$ cells have higher CD8α expression than WT T1 cells. Therefore, when we block CD8α, the cytolytic activity is lowered more substantially in T9$_{IL-33}$ cells than in T1 cells. Cytolytic activity of CD8α$^{-/-}$ T9$_{IL-33}$ cells was also decreased compared with that of WT T9$_{IL-33}$ cells (Fig. 9 H). Moreover, 85% of mice that received CD8α$^{-/-}$ T9$_{IL-33}$ cells died of leukemia (Fig. 9 I). Like murine T9$_{IL-33}$ cells, human T9$_{IL-33}$ cells exhibited enhanced expression of CD8α as well as GzmK, which correlates with CD8α up-regulation (Jung et al., 2013; Fig. 9 J). Blocking CD8α during human T9$_{IL-33}$ differentiation abolished their capacity to kill MOLM14 leukemic cells (Fig. 9 K). In summary, our data show that triggering mST2 on both murine and human T9 cells up-regulated CD8α expression and boosted the antileukemic activity of T9$_{IL-33}$ cells in vitro and in vivo.

DISCUSSION

Here, we show that the addition of IL-33 to IL-9–expressing CD4 (Th9) and CD8 (Tc9; together T9) cells enhanced their expression of mST2, IL-9, and PU.1. Compared with other T cell subsets that have been reported, T9 cells are not as well characterized. T9 cells arise after treatment with a cytokine combination of TGF-β1 and IL-4 (Dardalhon et al., 2008; Veldhoen et al., 2008). It has been shown that adding TGF-β1 to Th2 cells up-regulates mST2 expression (Blom et al., 2011). Consistent with this, we found that Th9 cells express higher levels of mST2. In addition, we show for the first time that Tc9 cells also have higher expression of mST2 and PU.1. PU.1 binds to the ST2 promoter and induces transcription of ST2 in mast cells and basophils (Baba et al., 2012), and it directly interacts with the IL-9 gene promoter, inducing IL-9 production (Chang et al., 2010) and inhibiting the production of Th2 cytokines (Chang et al., 2005). Although we did not study them here, other transcription factors and pathways such as BATF (Jabeen et al., 2013), IRF4 (Staudt et al., 2010; Tamiya et al., 2013), STAT5 (Olson et al., 2016), OX40/NF-κB (Xiao et al., 2012), and SIRT1–mTOR–HIF1α (Wang et al., 2016) have been shown to be important for optimal Th9 function. Determining the importance of these transcription factors and their possible regulation by IL-33 could help to even further tailor and strengthen the activity of T9$_{IL-33}$ cells.

vivo expression of Foxp3-GFP in gut CD4 T cells collected on day 14 after allo-HCT with either Foxp3-GFP–depleted or nondepleted allogeneic T9$_{IL-33}$ cells (n = 3, mean ± SEM). (I) Clinical scores of GVHD and survival curves for C3H.SW mice receiving B6 BM cells and in vitro differentiated Foxp3-GFP–depleted or nondepleted T9$_{IL-33}$ cells by flow cytometry (n = 9 per group, unpaired t test; data are shown as mean ± SEM).

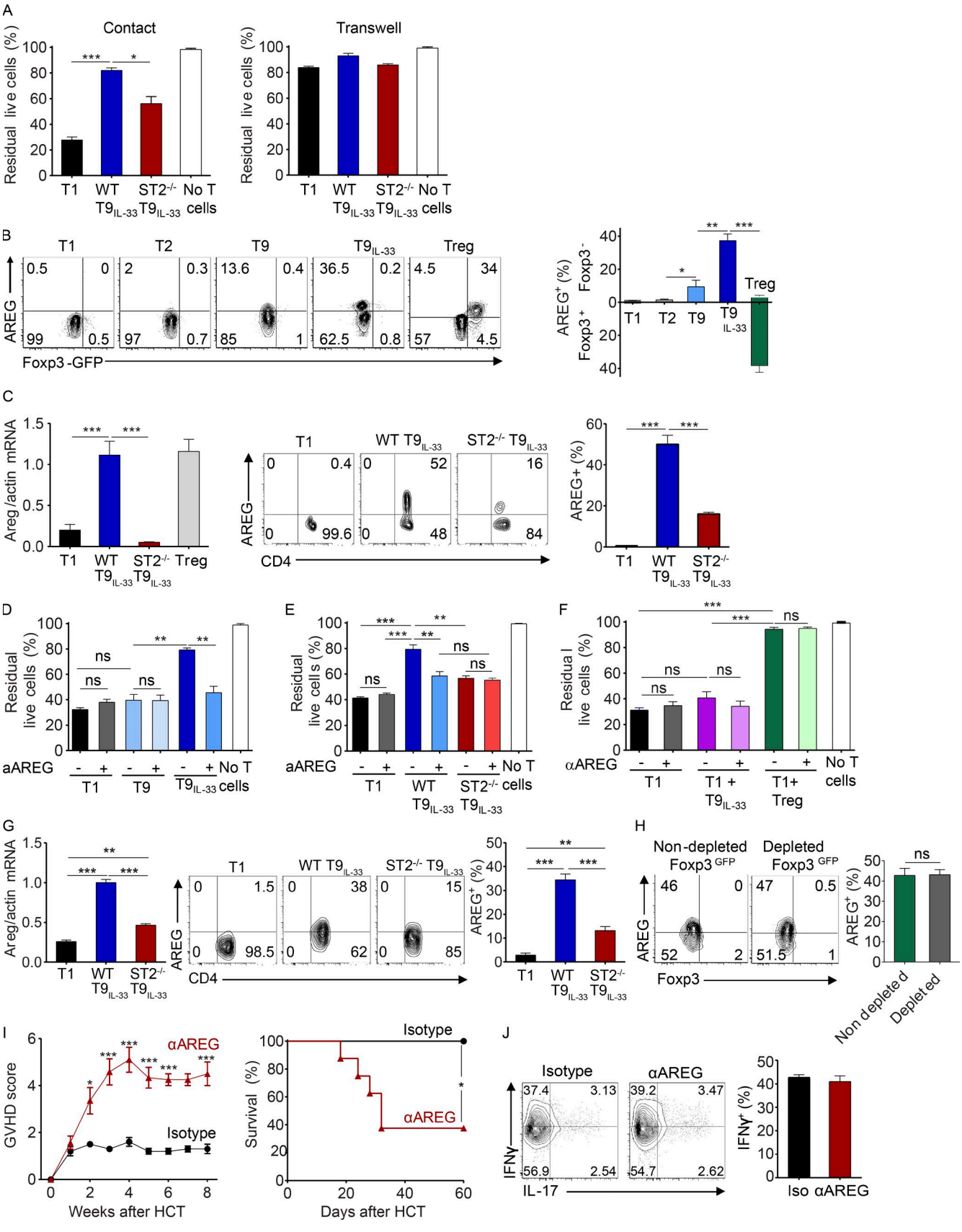

Acute GVHD is characterized by selective tissue damage to the mucosa, particularly of the gastrointestinal tract, and is driven mainly by donor T1 immune responses (van den Brink and Burakoff, 2002). ACT of in vitro T2 polarized allospecific donor T cells (Jung et al., 2003; Tawara et al., 2008) and Th2 and Th9 polarized cells in the presence of rapamycin (Mangus et al., 2013) decreased GVHD severity. Th2 cells showed a reduction in GVHD but were unable to control tumor cells in a murine model of L1210 leukemia, Jurkat T cell lymphoma, or metastatic breast cancer cell lines (Jung et al., 2013). Furthermore, in a phase 1 clinical trial, acute GVHD and overall survival were similar between Th2 and non-Th2 ACT recipients (Fowler et al., 2006). The impact of using both $CD4^+$ and $CD8^+$ T9 cells in GVHD and GVL had not been studied until now. We hypothesized that Th9 and Tc9 cells will behave like Th2 and Tc2 or T rapamycin in GVHD models while maintaining antileukemic activity in GVL models based on three studies showing that IL-9 and IL-9–producing T cells have potential as antitumoral therapies (Lu et al., 2012, 2014; Purwar et al., 2012). We used ACT because unlike many of the T cell subsets, it has been proven difficult to detect T9 cells in vivo, even in patients and models with Th2/Th9–driven diseases such as allergy (Kaplan et al., 2015; Kim et al., 2015). We nevertheless tried to enhance levels of in vivo murine T9 cells through the administration of TGF-β, IL-4, and IL-33 in donors or recipients, but we still observed a low frequency of T9 cells (unpublished data). One explanation for the difficulty in detecting these cells ex vivo is that T9 cells are short-lived. Another possibility is that T9 cells have high plasticity in vivo and become a different subset of T cell after injection. Further studies looking into the fate of adoptively transferred T9 and $T9_{IL\text{-}33}$ cells are warranted to determine what is happening to these cells after transfer. Even though our data clearly show a reduction in GVHD morbidity and mortality in murine models when using $T9_{IL\text{-}33}$ cells, similarly to Th2 cells, it is possible that this approach may not show efficacy in the clinic.

Mechanistically, our data show that mice receiving WT $T9_{IL\text{-}33}$ have lower levels of systemic soluble ST2 (sST2) accompanied with low levels of inflammatory cytokines (IFN-γ and TNF). The lower levels of soluble sST2 that we found could help explain the decrease in GVHD severity, as we have previously shown that sST2 is correlated with GVHD severity (Vander Lugt et al., 2013) and lowering sST2 levels using a blocking ST2 antibody ameliorated GVHD while preserving signaling through mST2 on T reg cells (Zhang et al., 2015). Indeed, studies have shown that IL-33 activation of $ST2^+$ T reg cells increases their suppressive function (Schiering et al., 2014; Zhang et al., 2015). Other studies have suggested that this increase in suppressive function of $ST2^+$ T reg cells can be explained by either up-regulation of IL-10 (Vasanthakumar et al., 2015) or AREG, independent of TCR signaling (Arpaia et al., 2015). It has recently been shown that periadministration of IL-33 expands recipient T reg cells that protect mice against acute GVHD (Matta et al., 2016). However, in vitro differentiation of $T9_{IL\text{-}33}$ cells did not results in any increase in T reg frequency, and ACT of $T9_{IL\text{-}33}$ cells did not lead to the accumulation of classical T reg cells or $ST2^+$ T reg cells. These results suggest that in our models, the phenotype we see is not a bystander effect but more dependent on a direct effect of $T9_{IL\text{-}33}$ cells on intestinal epithelial cells. IL-33 also promotes AREG expression on ILC2s, leading to intestinal tissue protection dependent on AREG–EGFR interactions (Monticelli et al., 2015). This AREG–EGFR interaction could explain

Figure 3. **ST2–IL-33 signaling enhances AREG expression on T9 cells, leading to protection of gut epithelial cells from alloreactivity.** (A) B6 T1, WT $T9_{IL\text{-}33}$, or $ST2^{-/-}$ $T9_{IL\text{-}33}$ cells differentiated in MLR conditions were co-cultured with BALB-5047 colonic epithelial cells together (left) or through Transwells (right) for 6 h. The percentage of residual live BALB-5047 cells was measured by viability dye staining negative and flow cytometry ($n = 4$ from two independent experiments, unpaired *t* test; data are shown as mean ± SEM). (B) Representative plots of AREG and Foxp3 expression on $CD4^+$ cells from in vitro differentiated T cell subsets from Foxp3-GFP reporter mice ($n = 3$, from three independent experiments, unpaired *t* test; data are shown as mean ± SEM; *, $P < 0.05$; **, $P < 0.01$; ***, $P < 0.001$). (C) AREG expression in in vitro differentiated and sorted CD4 subsets or T reg isolated freshly form spleen isolated magnetically using regulatory T cell isolation kit (Miltenyi). Gene expression was measured by real-time PCR and protein level by flow cytometry ($n = 3$, from three independent experiments, unpaired *t* test; data are shown as mean ± SEM; ***, $P < 0.001$). (D) Percentage of residual live cells of BALB-5047 cells after co-culture with T1, T9, or $T9_{IL\text{-}33}$ cells for 6 h in the presence of anti-AREG blocking antibody or isotype control ($n = 3$, from three independent experiments, unpaired *t* test; data are shown as mean ± SEM; **, $P < 0.01$). (E) Percentage of residual live cells of BALB-5047 cells after co-culture with T1, WT $T9_{IL\text{-}33}$, or $ST2^{-/-}$ $T9_{IL\text{-}33}$ cells for 6 h in the presence of anti-AREG blocking antibody or isotype control ($n = 3$, from three independent experiments, unpaired *t* test; data are shown as mean ± SEM; **, $P < 0.01$; ***, $P < 0.001$). (F) Percentage of residual live cells among BALB-5047 cells after co-culture with T1 cells, $T9_{IL\text{-}33}$ cells, T1 + $T9_{IL\text{-}33}$ cells, or T1 + in vitro polarized T reg cells (purified magnetically using the regulatory T cell isolation kit) for 6 h in the presence of anti-AREG blocking antibody or isotype control ($n = 3$, mean ± SEM). (G) AREG expression in sorted CD4 subsets from intestine of GVHD mice collected on day 14 after allo-HCT with T1, WT $T9_{IL\text{-}33}$, or $ST2^{-/-}$ $T9_{IL\text{-}33}$ cells ($n = 4$, unpaired *t* test; data are shown as mean ± SEM; ***, $P < 0.001$). (H) Representative plots of ex vivo expression of AREG and Foxp3 in gut CD4 T cells collected on day 14 after allo-HCT with allogeneic $T9_{IL\text{-}33}$ cells from Foxp3-GFP reporter mice depleted or nondepleted of Foxp3 T reg cells ($n = 3$, unpaired *t* test; data are shown as mean ± SEM). (I) Clinical scores of GVHD and survival curves for C3H.SW mice receiving B6 BM cells and in vitro differentiated $T9_{IL\text{-}33}$ cells treated with five doses of 100 µg anti-AREG or isotype control every other day from day −1 to day 7 ($n = 7$ per group, unpaired *t* test; data are shown as mean ± SEM; *, $P < 0.05$; ***, $P < 0.001$. For survival by log-rank test (**, $P < 0.01$; ***, $P < 0.001$.). (J) Representative plots of ex vivo IFN-γ and IL-17 expression by gut-infiltrating T cells 10 d after HCT in mice treated with αAREG or isotype control antibodies, and bar graphs showing frequencies of IFN-γ–positive T cells. B6 WT $T9_{IL\text{-}33}$ cells were cultured for 5 d, after which these cells were injected into lethally irradiated C3H.SW mice along with B6 WT BM cells. Mice were treated with a total of five doses of anti-AREG or isotype control (100 µg each) every other day from day −1 to day 7 ($n = 4$, unpaired *t* test; data are shown as mean ± SEM).

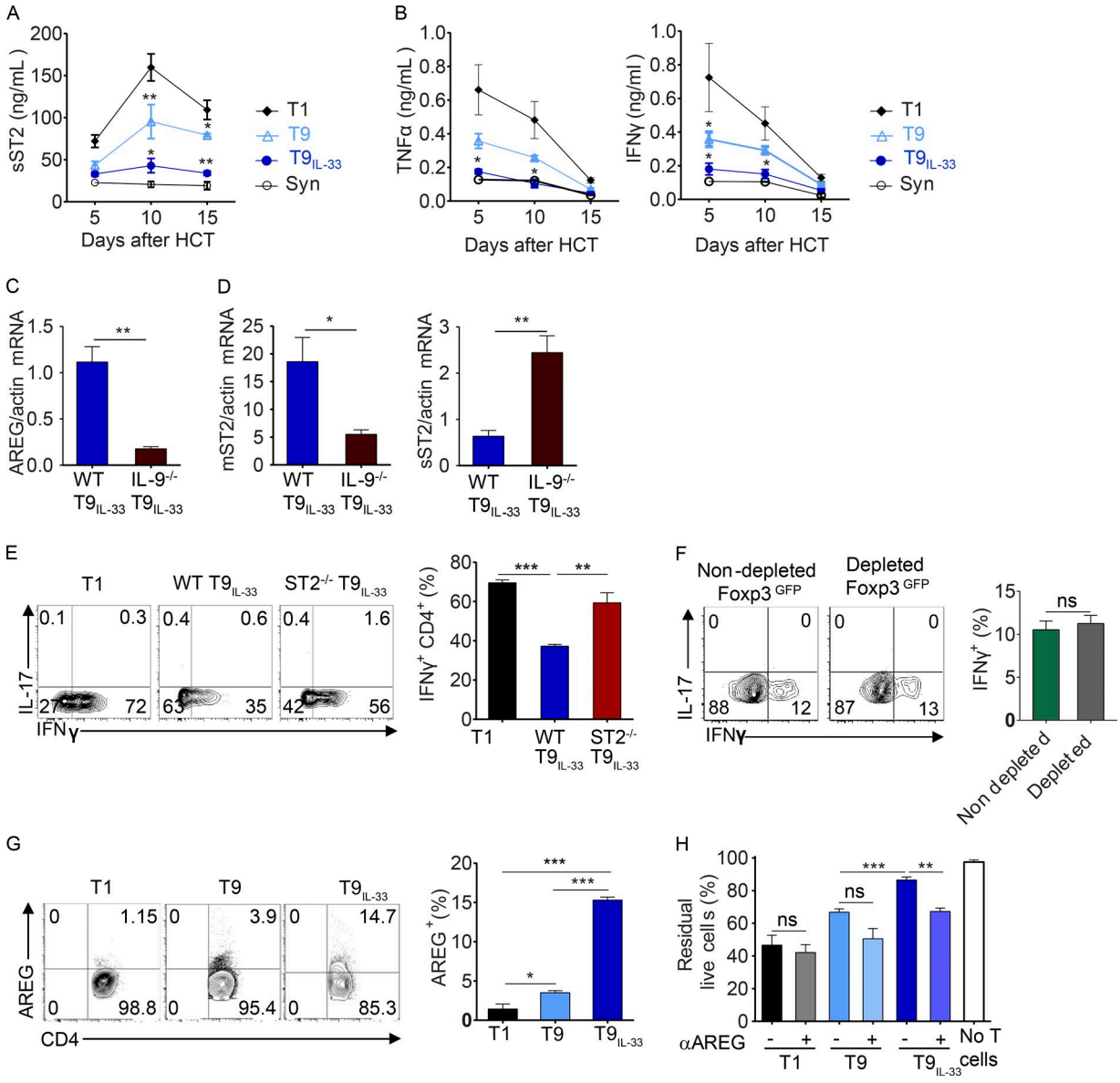

Figure 4. **Allogeneic T cell interaction with colonic epithelial cells and AREG blockade in mice and human.** (A) sST2 concentration in plasma collected every 5 d after HCT from the BALB/c mice receiving 5 × 10^6 BM cells plus 10^6 from (n = 4, from two independent experiments, unpaired t test; data are shown as mean ± SEM; *, P < 0.05; **, P < 0.01). (B) TNF and IFN-γ concentrations in plasma collected every 5 d after HCT from BALB/c mice receiving 5 × 10^6 BM cells plus 1 × 10^6 from syngeneic T cells (BALB/c mice) or T1, T9, or $T9_{IL-33}$ T cells from B6 WT mice (n = 4, from two independent experiments, unpaired t test; data are shown as mean ± SEM; *, P < 0.05, **. P < 0.01). (C) Ratio of AREG/actin mRNA expression in WT or IL-$9^{-/-}$ $T9_{IL-33}$ cells. (D) Ratio of mST2/actin expression (left) and sST2/actin expression (right) in WT or IL-$9^{-/-}$ $T9_{IL-33}$ cells (n = 3, from three independent experiments, unpaired t test; data are shown as mean ± SEM; *, P < 0.05; **, P < 0.01). (E) Ex vivo expression of IFN-γ and IL-17 in gut CD4 T cells collected on day 14 after allo-HCT with allogeneic T1, WT $T9_{IL-33}$, or $ST2^{-/-}$ $T9_{IL-33}$ cells (n = 4, from two independent experiments, unpaired t test; data are shown as mean ± SEM; **, P < 0.01; ***, P < 0.001). (F) Ex vivo expression of IFN-γ and IL-17 in gut CD4 T cells collected on day 14 after allo-HCT with $T9_{IL-33}$ cells from Foxp3-GFP reporter mice depleted or nondepleted of Foxp3 T reg cells (n = 3, unpaired t test; data are shown as mean ± SEM). (G) AREG expression on in vitro differentiated human T1, T9, and $T9_{IL-33}$ CD4 cells from healthy donors (n = 3, from three independent experiments, unpaired t test; data are shown as mean ± SEM; *, P < 0.05; **, P < 0.01; ***, P < 0.001). (H) Percentage of residual live human colonic cells after co-culture with T1, T9, $T9_{IL-33}$ cells for 6 h in the presence of anti-AREG blocking antibody or isotype control and without T cells as control (n = 3, from three independent experiments, unpaired t test; data are shown as mean ± SEM; **, P < 0.01; ***, P < 0.001).

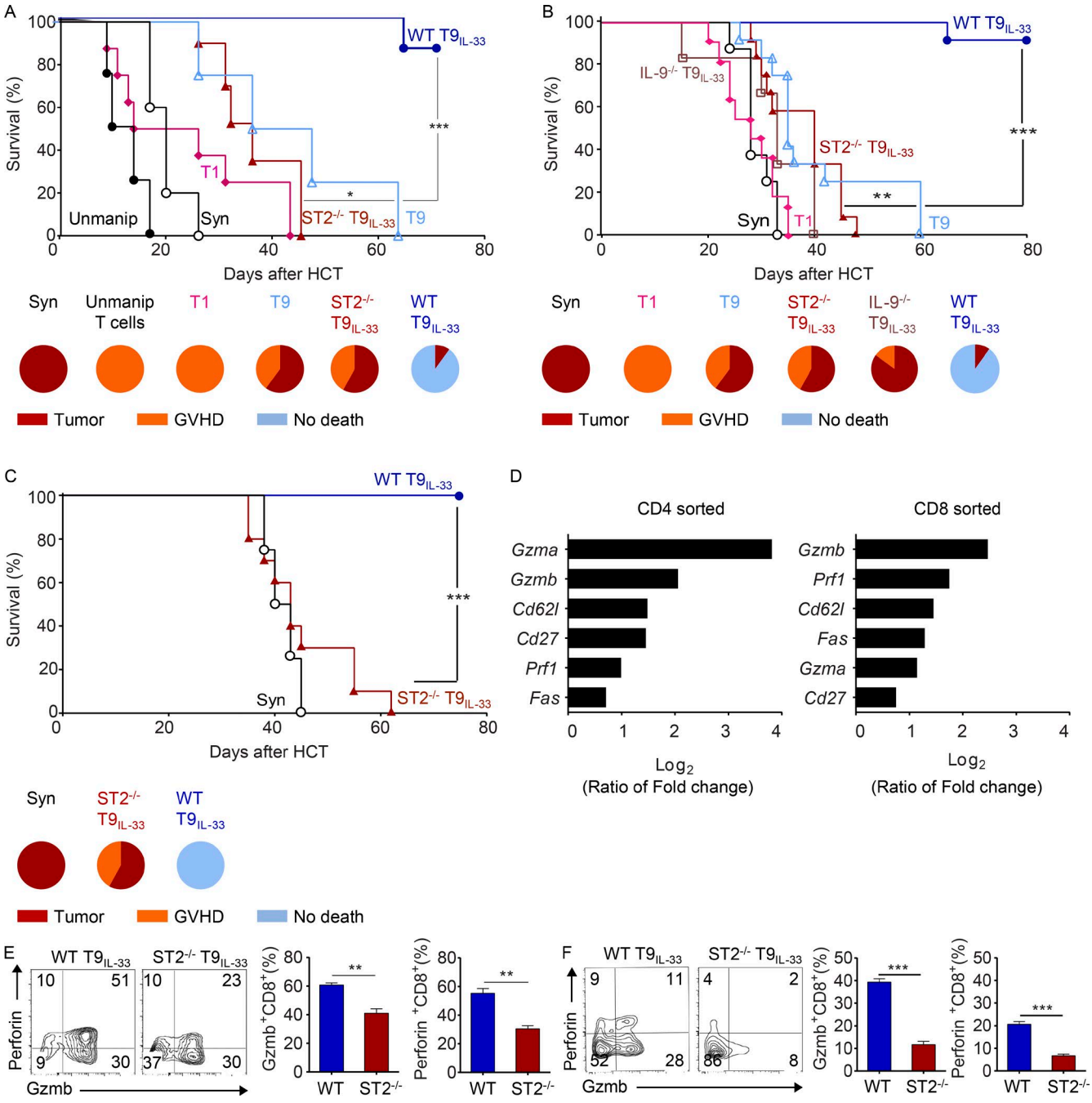

Figure 5. **$T9_{IL-33}$ cells preserve GVL and antitumor activity.** (A). Survival curves for BALB/c mice receiving 10^4 syngeneic lymphoma cell line A20 cells with syngeneic T cells or allogeneic in vitro differentiated cells (n = 12 mice per group, from two independent experiments; ***, P < 0.0001, log-rank test). Pie charts show cause of death. (B) Survival curves for BALB/c mice receiving 10^4 cells of the syngeneic MLL-AF9 leukemic cell line with syngeneic T cells or allogeneic in vitro differentiated cells (n = 12 mice per group, from two independent experiments; **, P < 0.01; ***, P < 0.001, log-rank test). Pie charts show cause of death. (C) Survival curves for C3H.SW mice receiving 10^4 MLL-AF9 leukemic cells with syngeneic $T9_{IL-33}$ cells or allogeneic in vitro differentiated cells (n = 14 mice per group, from two independent experiments; ***, P < 0.001, log-rank test). Pie charts show cause of death. (D) Transcriptome analysis of *Gzma*, *Gzmb*, *Prf1*, *Cd62l*, *Cd27*, and *Fas* expression in sorted WT $T9_{IL-33}$ versus $ST2^{-/-}$ $T9_{IL-33}$ CD8 and CD4 cells (n = 3; see Fig. S2). (E) Representative plots of Gzmb and Prf1 expression in WT $T9_{IL-33}$ and $ST2^{-/-}$ $T9_{IL-33}$ cells gated on CD8, and bar graphs showing the frequency of $GzmB^+$ and $Prf1^+$ CD8 T cells (n = 8, from four independent experiments, unpaired t test; data are shown as mean ± SEM; **, P < 0.01). (F) Representative plots of GzmB and Prf1 expression in gated CD8 T cells from BM 28 d after adoptive transfer of allogeneic T cells with syngeneic MLL-AF9 cells. Bar graphs show the frequency of $GzmB^+$ and $Prf1^+$ CD8 T cells (n = 4, unpaired t test; data are shown as mean ± SEM; ***, P < 0.001).

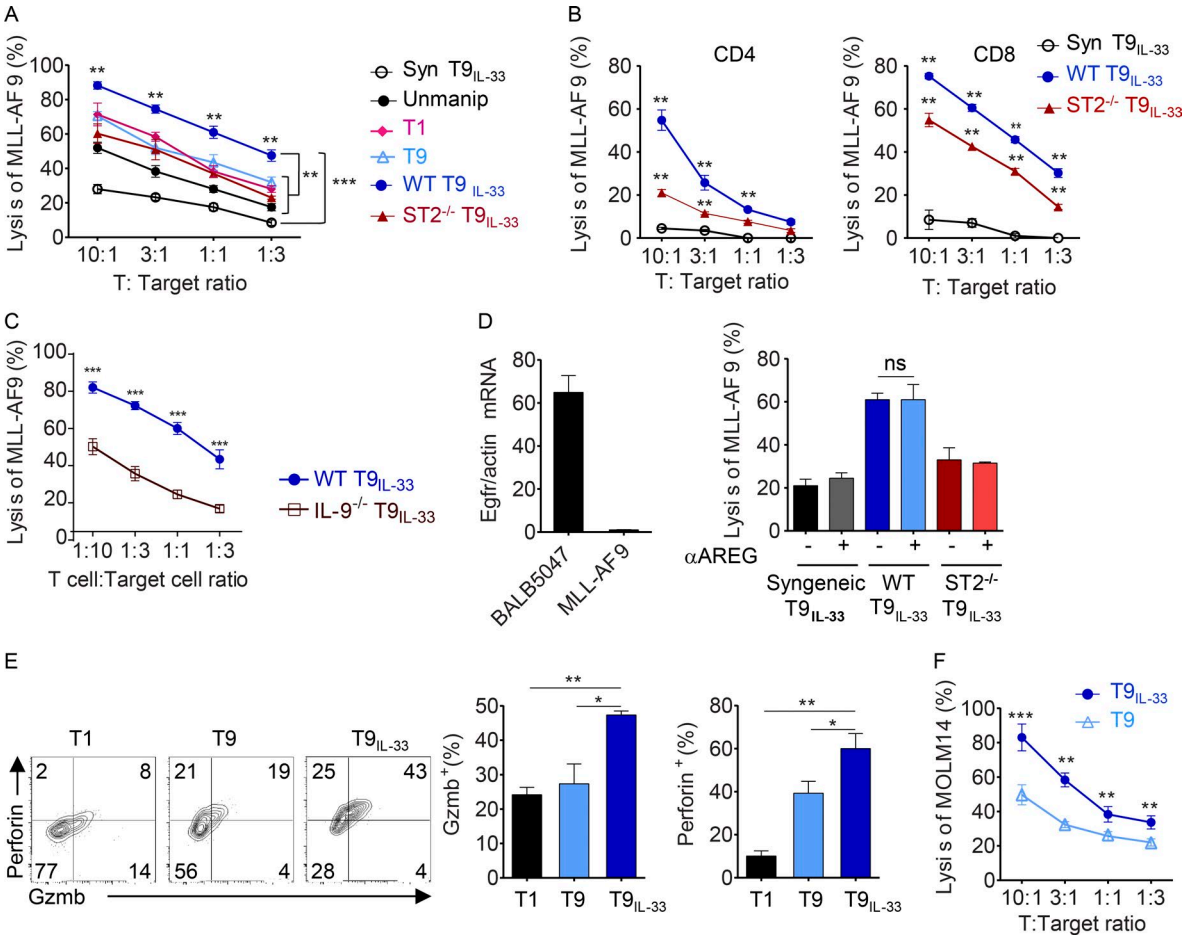

Figure 6. **ST2–IL-33 signaling enhances cytolytic molecules expression and cytolytic activity.** (A) Cytolytic assays: B6 or C3H.SW T cell MLR cultures were co-cultured with C3H.SW-derived MLL-AF9 leukemic cells for 6 h ($n = 4$, from two independent experiments, unpaired t test; data are shown as mean ± SEM; **, $P < 0.01$). (B) Cytolytic assays. CD4 or CD8 purified from B6 or C3H.SW T cell MLR cultures were co-cultured with C3H.SW-derived MLL-AF9 cells for 6 h ($n = 4$, from four independent experiments, unpaired t test; data are shown as mean ± SEM; **, $P < 0.01$). (C) Cytolytic assay of B6 WT or IL-$9^{-/-}$ $T9_{IL-33}$ cells differentiated under MLR conditions. After 5 d, WT or IL-$9^{-/-}$ $T9_{IL-33}$ cells were incubated with BALB/c MLL-AF9 cells for 6 h ($n = 3$, from three independent experiments, unpaired t test; data are shown as mean ± SEM; ***, $P < 0.001$). (D) mRNA expression of *Egfr* on BALB-5047, MLL-AF9 cells by quantitative PCR (left). Syngeneic $T9_{IL-33}$, WT $T9_{IL-33}$, or $ST2^{-/-}$ $T9_{IL-33}$ cells were differentiated in MLR conditions and co-cultured with BALB/c MLL-AF9 cells for 6 h at a ratio of 10:1 with anti-AREG (right; $n = 3$, unpaired t test; data are shown as mean ± SEM). (E) Representative plots of human GzmB and perforin expression in human T9 and $T9_{IL-33}$ cells, and bar graphs showing the frequencies of $GzmB^+$ and $GzmK^+$ cells ($n = 3$, from three independent experiments, unpaired t test; data are shown as mean ± SEM; *, $P < 0.05$; **, $P < 0.01$). (F) Cytolytic assays of human T9 or $T9_{IL-33}$ cells incubated for 6 h with MOLM14 leukemia cells ($n = 3$, from three independent experiments, unpaired t test; data are shown as mean ± SEM; **, $P < 0.01$; ***, $P < 0.001$).

why ILC2s were associated with reduced susceptibility to GVHD in 51 acute leukemia patients, but their reconstitution after allo-HCT was slow (Munneke et al., 2014). ACT of $T9_{IL-33}$ cells in our acute models of GVHD did not lead to the accumulation of ILC2s in the gut, again suggesting a direct effect of $T9_{IL-33}$ on intestinal epithelial cells. We then showed that $T9_{IL-33}$ cells have a direct contact-dependent effect on intestinal epithelial cells. AREG expression on $T9_{IL-33}$ cells was the reason for their GVHD protective effect, as has been shown for T reg cells and ILC2s (Arpaia et al., 2015; Monticelli et al., 2015), but not other T cell subsets. Indeed, our data showed that $T9_{IL-33}$ cells express high levels of AREG like T reg cells, and this expression was maintained on infiltrated T cells in the gut after allo-HCT. AREG expression on $T9_{IL-33}$ cells was independent of Foxp3 expression in vitro and in vivo. Furthermore, blocking AREG on $T9_{IL-33}$ cells reduced allogeneic mouse and human colonic epithelial survival in vitro and increased GVHD severity in vivo. This led to a reduction in the frequency of pathogenic Th1 cells in the intestine. This reduction of Th1 response ex vivo is mediated by high expression of mST2 and low levels of sST2, as we previously described (Zhang et al., 2015). Foxp3 depletion from $T9_{IL-33}$ cell cultures before ACT did not have any impact on the protective effect of $T9_{IL-33}$ cells in GVHD. Together,

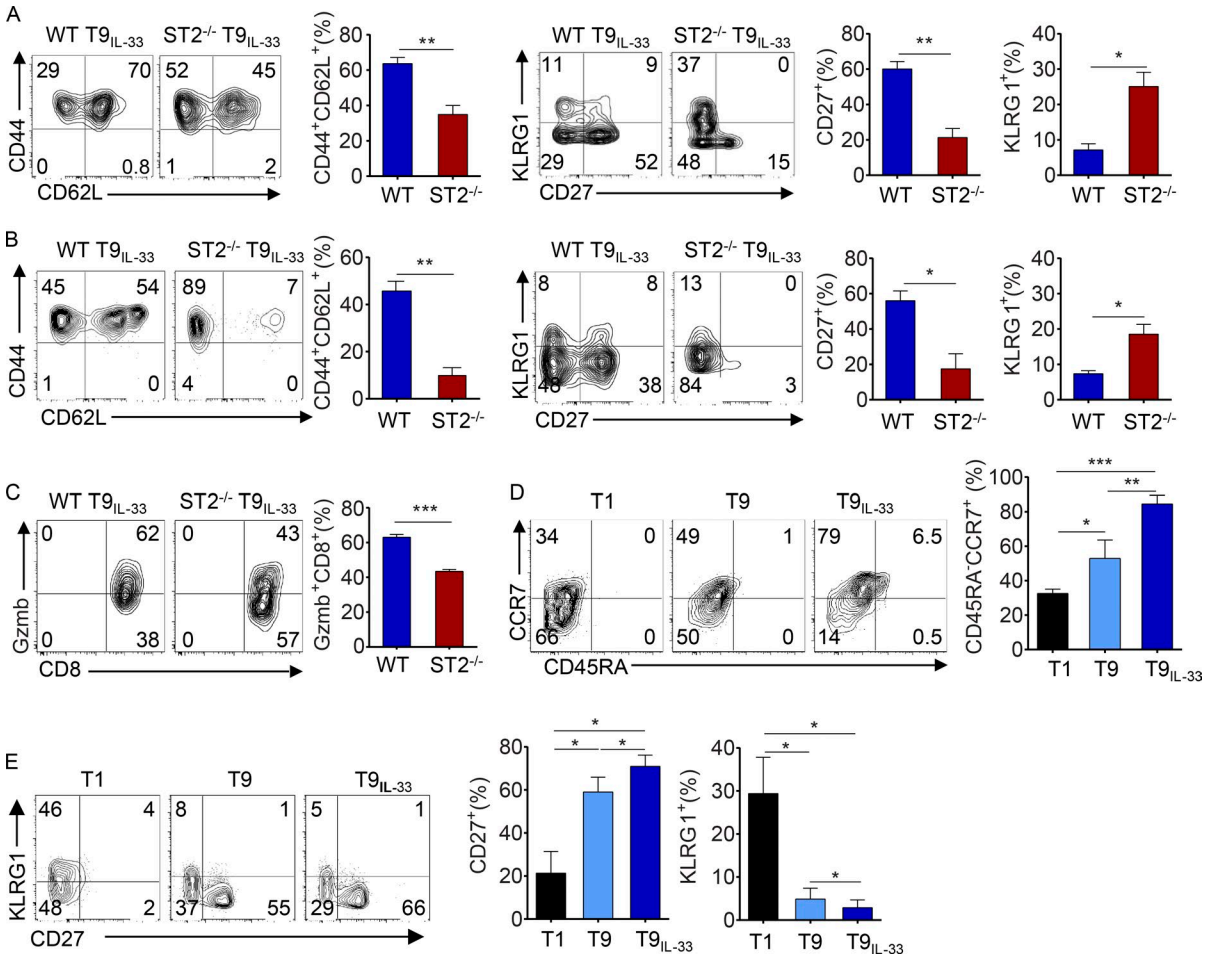

Figure 7. **ST2–IL-33 signaling preserves central memory phenotype.** (A) Representative plots of CD62L$^+$ and CD44$^+$ (left) and CD27$^+$ and KLRG1$^+$ (right) cells, and bar graphs showing the frequency of CD44$^+$CD62L$^+$, CD27$^+$, and KLRG1$^+$ CD8 T cells from in vitro differentiated cells from WT $T9_{IL-33}$ versus ST2$^{-/-}$ $T9_{IL-33}$ cells (n = 4, from four independent experiments, unpaired t test; data are shown as mean ± SEM; **, P < 0.01). (B) Representative plots of CD62L$^+$ and CD44$^+$ (left) and CD27$^+$ and KLRG1$^+$ (right) cells, and bar graphs showing the frequency of CD44$^+$CD62L$^+$ and CD27$^+$ CD8 T cells from ex vivo BM collected on day 28 from mice receiving MLL-AF9 leukemic cells with WT $T9_{IL-33}$ or ST2$^{-/-}$ $T9_{IL-33}$ cells (n = 4, unpaired t test; data are shown as mean ± SEM; *, P < 0.05; **, P < 0.01). (C) Representative plots of Gzmb expression in WT or ST2$^{-/-}$ CD8$^+$KLRG-1$^+$CD27$^-$ short-term effector cells differentiated under $T9_{IL-33}$ conditions, and a bar graph showing the frequency of Gzmb expression in these cells (n = 3, unpaired t test; data are shown as mean ± SEM; ***, P < 0.001). (D and E) Representative plots of CD45RA$^-$ and CCR7$^+$ (D) and CD27$^+$ and KLRG1$^+$ (E) cells, and bar graphs showing the frequency of CD45RA$^-$CCR7$^+$, CD27$^+$, and KLRG1$^+$ CD8 T cells from in vitro differentiated T1, T9, and $T9_{IL-33}$ human cells (n = 3, from three independent experiments, paired t test; data are shown as mean ± SEM; *, P < 0.05; **, P < 0.01).

our data show that in our models, the protective phenotype of intestinal epithelial cells from alloreactivity is directly dependent on AREG-positive $T9_{IL-33}$ cells. Therefore, possible avenues for exploring the ST2–IL-33 pathway as a target for GVHD treatment include blockade of sST2 through loss of IL-33 sequestration by sST2 (Zhang et al., 2015) and ACT of mST2-expressing $T9_{IL-33}$ cells through protection by AREG–EGFR signaling.

Although new therapeutic approaches such as chimeric antigen receptor T cells have shown promise in acute and chronic lymphoid leukemias (Grupp et al., 2013; Porter et al., 2015), their use in AML requires subsequent HCT due to myelotoxicity to normal cells (Kenderian et al., 2015). Allogeneic specific T cells can be generated without gene transfer and exhibit adequate T cell receptor affinity (Bachireddy et al., 2015; Cruz and Bollard, 2015; Dotti, 2015), but unfortunately, their reactivity to alloantigens in normal host tissues often leads to GVHD. Furthermore, most experimental strategies to separate GVHD and GVL responses merely spare GVL function without enhancing it. Th1 and Tc1 cells have been regarded as most efficient in tumor rejection among the subsets of T cells (Dunn et al., 2006); however, ACT therapy of Tc1 had limited success, because high expression of T-bet led to a short life span (Joshi et al., 2007) and exhausted phenotype of these cells via up-regulation of KLRG1, PD-1, LAG3, and 2B4 (Crespo et al., 2013). One explanation for

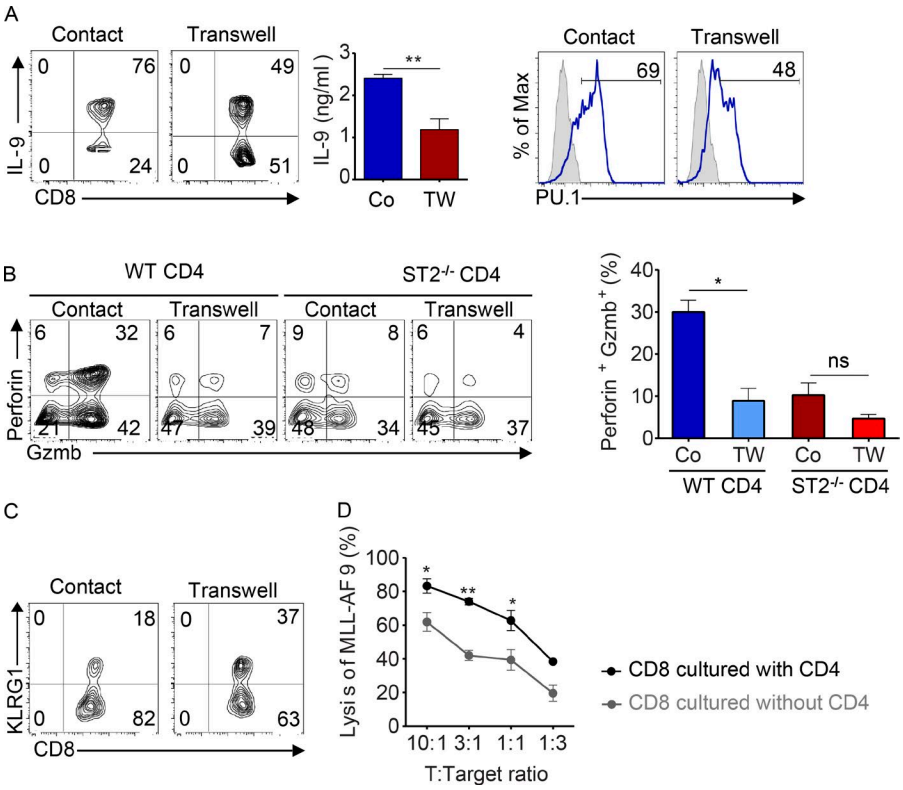

Figure 8. **ST2–IL-33 signaling in CD4 impacts CD8 antitumor activity.** (A) Granzyme B and perforin expression in CD8 T cells cultured with WT or ST2$^{-/-}$ CD4 cells together or through a Transwell under T9$_{IL-33}$ conditions (n = 3, from three independent experiments, unpaired t test; data are shown as mean ± SEM; *, P < 0.05). (B) Splenic CD4 and CD8 cells were either co-cultured together or separated in a Transwell under T9$_{IL-33}$ conditions for 5 d. Representative plots and mean ± SEM of IL-9 expression in CD8 T cells (left), IL-9 secretion from total T9$_{IL-33}$ (center), and PU.1 expression in CD8 T cells (right) either from co-culture (Co) or through Transwell (TW; n = 3, unpaired t test; data are shown as mean ± SEM; **, P < 0.01). (C) KLRG1 expression on CD8 cells cultured together or through a Transwell with CD4 T cells. (D) Cytolytic assays of purified CD8 cells differentiated into Tc9$_{IL-33}$ cells or co-cultured in the presence of CD4 in MLR conditions (n = 4, from two independent experiments, unpaired t test; data are shown as mean ± SEM; *, P < 0.05).

these differences between T1 and T9$_{IL-33}$ cells might be due to the reduced IFN-γ production by T9$_{IL-33}$ cells. The presence of high amounts of IFN-γ has been shown to up-regulate exhaustion markers and induce apoptosis of late effector memory phase T cells (Badovinac et al., 2000; Joshi et al., 2007). The GVL activity of T9$_{IL-33}$ cells could also be explained by the persistence of their central memory phenotype, which has been shown to enhance antitumor activity (Klebanoff et al., 2005, 2016). Recently, it has been shown that IRF1–IL-21 signals and GITR signaling increases antitumor activity of T9 cells in melanoma models (Végran et al., 2014; Kim et al., 2015); however, we did not observe any difference at transcript levels of IL-21, IRF1, and GITR between CD4 and CD8 WT or ST2$^{-/-}$ T9$_{IL-33}$ cells (Table S2). Further studies need to be completed to better understand how T9$_{IL-33}$ cells maintain their central memory phenotype without becoming exhausted.

On CD8 T cells, ST2–IL-33 signaling drives protective antiviral responses (Bonilla et al., 2012). We showed here that ST2–IL-33 signaling enhanced antitumor CD8$^+$ T cell responses. The absence of CD4 T cells generates corrupt CD8 effector T cells (Ghosh et al., 2016). We showed here that Th9 cells license Tc9 for expression and production of ST2, IL-9, cytolytic molecules, and killing via a contact-dependent ST2–IL-33 pathway for optimal activity. Different mechanisms have been shown to explain the importance of CD4 T cells for antitumor activity of CD8 T cells. One of these mechanisms was the interaction between CD4 and CD8 via OX40 (Song et al., 2007). OX40 expression has been shown to be up-regulated on Th2 upon IL-33 activation (Murakami-Satsutani et al., 2014) and enhanced in Th9 cells (Xiao et al., 2012). We also noted significant up-regulation of OX40 (Tnfrsf4; Table S2) in both CD4 and CD8 WT T9$_{IL-33}$ cells compared with CD4 and CD8 ST2$^{-/-}$ T9$_{IL-33}$ cells. Furthermore, we observed an ST2–IL-33–dependent increase in CD8α expression on both CD4 and CD8 T9$_{IL-33}$ cells. Mutation of the CD8α subunit leads to the deficiency of all CD8 T cell differentiation in the thymus (Kang et al., 2010) and impairs the development of cytotoxic T cell function (Fung-Leung et al., 1991) as well as antitumoral activity (de la Calle-Martin et al., 2001). Therefore, the T cell cytotoxic function is difficult to induce in absence of CD8a T cells, but it can be rescued by simultaneous removal of MHCII, consequently removing CD8 T cells and allowing for diminished competitiveness (Riddle et al., 2008). We found that blocking CD8α or use of CD8α KO animals completely abolished the antitumor activity of T9$_{IL-33}$ cells. CD8α up-regulation has been associated with up-regulation of GzmK and massive infiltration of CD8 T cells in the stroma of patients with HPV1 oropharyngeal squamous cell carcinoma that correlated with prolonged survival (Jung et al., 2013). We also detected an increase in the production of GzmK correlated with CD8α expression on human Tc9$_{IL-33}$ cells. There are no published data on GzmK expression in murine T cells and/or its relation with CD8α. Further studies of this important antitumoral mechanism are required. We demonstrated that

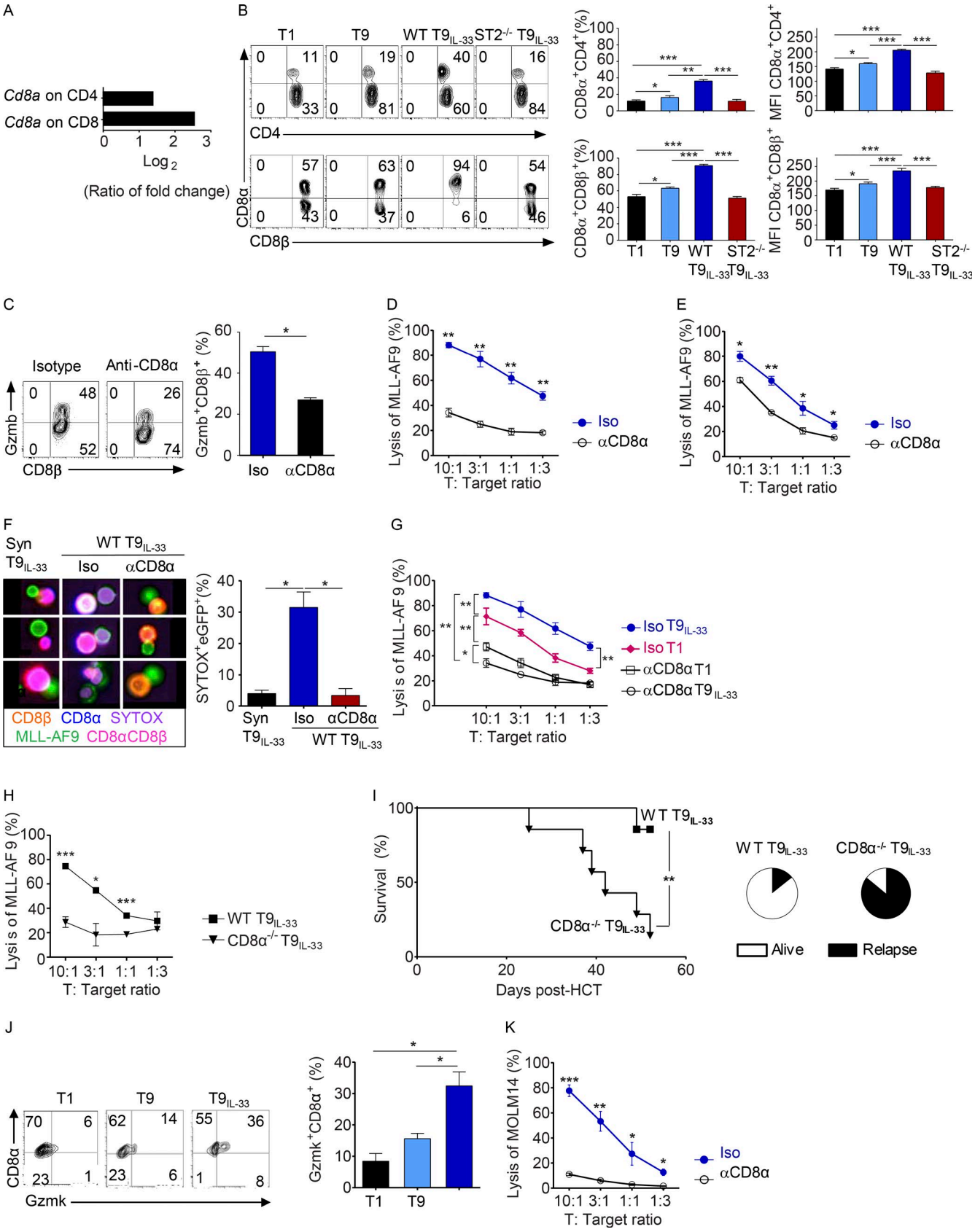

knocking down IL-9 decreased antitumor activity both in vitro and in vivo through activation of ST2–IL-33 signaling. Expression of ST2–IL-33 increases the levels of IL-9, CD8α, and cytolytic molecule expression and preserves the central memory phenotype of these Tc9 cells, leading to increased antitumor activity of T9 cells.

We conclude that ST2–IL-33 activation of both murine and human IL-9–secreting T cells may serve as a new T cell therapy with dual opposing mechanisms: protecting normal tissues through up-regulation of AREG and mediating antileukemic activity via CD8α expression. Therefore, ACT of allogeneic $T9_{IL\text{-}33}$ cells offers an attractive approach for separating GVL activity from GVHD.

MATERIALS AND METHODS

Mice

BALB/c (H-2^d), C57BL/6 (B6, H-2^b, CD45.2^+), C57BL/6. Ptprca (B6-SJL, H-2^b, CD45.1^+), C3H.SW (H-2^b, CD45.2^+), and B6.129S2-Cd8atm1Mak/J (H-2^b, CD45.2) mice were purchased from The Jackson Laboratory. B6 $ST2^{-/-}$ (CD45.2^+) mice were provided by A. McKenzie (University of Cambridge, Cambridge, England, UK), and B6 $IL\text{-}9^{-/-}$ (CD45.2^+) mice were provided by A. Rosenkranz (University of Graz, Graz, Austria). Animal protocols were approved by the Institutional Animal Care and Use Committee at Indiana University School of Medicine.

T cell differentiation

Total, $CD4^+$, and $CD8^+$ T cells were purified from spleens via magnetic bead selection (Miltenyi Biotec). Cells were plated at a concentration of 1×10^6 cells/ml and activated with 1 μg/ml plate-bound anti-CD3 (2C11) and 5–10 μg/ml soluble anti-CD28 (37.51). $CD4^+$ and $CD8^+$ cells were polarized toward T0 (without cytokines), T1 (1 ng/ml IL-2 and 20 ng/ml IL-12), T2 (20 ng/ml IL-4), T9 (4 ng/ml TGF-β and 10 ng/ml IL-4), or $T9_{IL\text{-}33}$ (4 ng/ml TGF-β, 10 ng/ml IL-4, and 10 ng/ml IL-33) in DMEM supplemented with 10% FBS, 2 mM L-glutamine, 1% penicillin/streptomycin, 1 mM sodium pyruvate, and 50 μM β-mercaptoethanol (Life Technologies). On day 3, cells were expanded with fresh growth media in the presence of additional cytokines at the same concentrations as in day 0 medium. On day 5, cells were collected, washed, and prepared for phenotypic analysis or ACT into recipient mice.

Human T cells ($CD4^+$ or $CD8^+$) were purified from PBMCs of healthy donors and activated with anti–CD3/CD28 microbeads (Life Technologies). Both $CD4^+$ and $CD8^+$ cells were polarized toward T1 (1 ng/ml IL-2 and 20 ng/ml IL-12), T2 (20 ng/ml IL-4), T9 (4 ng/ml TGF-β and 10 ng/ml IL-4), or $T9_{IL\text{-}33}$ (4 ng/ml TGF-β, 10 ng/ml IL-4, and 10 ng/ml IL-33) in complete RPMI medium with 10% human AB serum. On day 3, cells were expanded with fresh medium in the presence of additional cytokines at the same concentrations as on day 0. On day 7, cells were collected, washed, and prepared for phenotypic analysis and in vitro assays.

Induction and assessment of GVHD

Mice underwent allo-BM transplantation as previously described (Zhang et al., 2015). In brief, BALB/c and C3H.SW recipients received 900 and 1100 cGy total body irradiation (^{137}Cs source), respectively, on day -1. Recipient mice were injected intravenously with 5×10^6 T cell–depleted (TCD) BM cells plus in vitro differentiated T0, T1, T2, T9, WT $T9_{IL\text{-}33}$, $ST2^{-/-}$ $T9_{IL\text{-}33}$, or $IL\text{-}9^{-/-}$ $T9_{IL\text{-}33}$ T cells (1×10^6 for BALB/c and 3×10^6 for C3H.SW) from either syngeneic or allogeneic donors at day 0. TCD BM cells from donors were prepared with CD90.2 Microbeads (Miltenyi Biotec). Mice were housed in sterilized microisolator cages and maintained on acidified water (pH <3) for 3 wk. Survival was monitored daily, and clinical GVHD scores were assessed weekly as de-

Figure 9. **CD8α expression is up-regulated on $CD4^+$ and $CD8^+$ murine and human $T9_{IL\text{-}33}$ cells and increases their killing of leukemia cells.** (A) Transcriptome analysis of CD8α expression in sorted WT $T9_{IL\text{-}33}$ versus $ST2^{-/-}$ $T9_{IL\text{-}33}$ CD8 and CD4 cells ($n = 3$; see Fig. S2). (B) Representative plots of CD8α expression on $CD4^+$ (top) and $CD8\beta^+$ (bottom) T cells from in vitro differentiated murine T1, T9, WT $T9_{IL\text{-}33}$, and $ST2^{-/-}$ $T9_{IL\text{-}33}$ cells, and bar graphs showing the frequency and mean florescence intensity (MFI) of $CD4^+CD8a^+$ and $CD8\alpha^+CD8\beta^+$ T cells for each condition ($n = 6$, from three independent experiments, unpaired *t* test; data are shown as mean ± SEM; *, $P < 0.05$; **, $P < 0.01$; ***, $P < 0.001$). (C) Representative plots of Gzmb expression in $CD8\beta^+$ T cells differentiated under $T9_{IL\text{-}33}$ conditions plus either anti-CD8α or isotype control, and bar graphs showing the frequency of $Gzmb^+CD8\beta^+$ cells ($n = 3$, from three independent experiments, unpaired *t* test; data are shown as mean ± SEM; *, $P < 0.05$). (D) Cytolytic assays of in vitro differentiated B6 $T9_{IL\text{-}33}$ incubated with BALB/c MLL-AF9 cells in the presence of anti-CD8α or isotype control for 6 h ($n = 3$, from three independent experiments, unpaired *t* test; data are shown as mean ± SEM; **, $P < 0.01$). (E) Cytolytic assays. B6 $T9_{IL\text{-}33}$ cells were differentiated in MLR conditions with anti-CD8α blocking antibody or isotype control. After 5 d, $T9_{IL\text{-}33}$ cells were incubated with BALB/c MLL-AF9 cells for 6 h ($n = 3$, from three independent experiments, unpaired *t* test; data are shown as mean ± SEM; *, $P < 0.05$; **, $P < 0.01$). (F) ImageStream cell images of syngeneic $T9_{IL\text{-}33}$ or allogeneic $T9_{IL\text{-}33}$ cells incubated with BALB/c eGFP–MLL-AF9 cells and anti-CD8α blocking antibody or isotype control for 3 h ($n = 3$, unpaired *t* test; data are shown as mean ± SEM; *, $P < 0.05$). (G) Cytolytic assays of in vitro differentiated B6 T1 or $T9_{IL\text{-}33}$ incubated with BALB/c MLL-AF9 cells in the presence of anti-CD8α or isotype control for 6 h ($n = 3$, mean ± SEM). (H) Cytolytic assay of in vitro differentiated B6 WT $T9_{IL\text{-}33}$ or $CD8\alpha^{-/-}$ $T9_{IL\text{-}33}$ cells in MLR conditions. After 5 d, both WT and $ST2^{-/-}$ $T9_{IL\text{-}33}$ cells were incubated with BALB/c MLL-AF9 cells for 6 h ($n = 3$, unpaired *t* test; data are shown as mean ± SEM; *, $P < 0.05$; ***, $P < 0.001$). (I) Survival curves for BALB/c mice receiving 10^4 cells of the syngeneic MLL-AF9 leukemic cell line with allogeneic WT ($n = 7$ mice per group, **, $P < 0.01$, log-rank test). Pie charts show relapses. (J) Representative plots of CD8α and GzmK expression from human in vitro differentiated T1, T9, and $T9_{IL\text{-}33}$ cells and a bar graph showing the frequency of $GzmK^+CD8\alpha^+$ T cells from each condition ($n = 3$, from three independent experiments, unpaired *t* test; data are shown as mean ± SEM; *, $P < 0.05$). (K) Cytolytic assays of human $T9_{IL\text{-}33}$ cells differentiated with anti-CD8α blocking antibody or isotype control and incubated with MOLM14 cells for 6 h ($n = 3$, from three independent experiments, unpaired *t* test; data are shown as mean ± SEM; *, $P < 0.05$; **, $P < 0.01$; ***, $P < 0.001$).

scribed previously (Cooke et al., 1996). Mice were euthanized when the clinical scores reached 6.5, in accordance with animal protocols approved by the institutional review board.

Induction and assessment of the GVL effect

BALB/c or C3H.SW mice were lethally irradiated (900 or 1,100 cGy, respectively) on day −1. Recipient mice were injected intravenously on day 0 with 5×10^6 syngeneic or allogeneic TCD BM cells and in vitro differentiated syngeneic $T9_{IL\text{-}33}$ cells or T0, T1, T9, or $T9_{IL\text{-}33}$ from WT B6 mice, or $T9_{IL\text{-}33}$ from $ST2^{-/-}$ B6 mice at 1×10^6 T cells for BALB/c recipient mice or 3×10^6 T cells for C3H.SW recipient mice. For GVL experiments, syngeneic GFP–MLL-AF9 leukemic cells generated from C3H.SW or BALB/c BM, as described previously (Zhang et al., 2015), were injected on day 0 at 1×10^4 GFP–MLL-AF9 cells for each recipient mice as well. Mice were monitored daily for survival and leukemia development, and GVHD was scored weekly. We attributed death to leukemia based on a high percentage of $eGFP^+$ cells and death to GVHD only if the mice had a low percentage of $eGFP^+$ cells and a GVHD score ≥6.5. Cells from peripheral blood, BM, spleen, and liver were analyzed by flow cytometry.

In vitro cytotoxicity assay

Purified splenic T cells were primed in a mixed lymphocyte reaction (MLR) in the presence of polarizing cytokines (IL-4, TGF-β, and IL-33) for 5 d. Total $T9_{IL\text{-}33}$ cells or sorted CD4 and CD8 from B6 WT $T9_{IL\text{-}33}$, $ST2^{-/-}$ $T9_{IL\text{-}33}$, or C3H.SW $T9_{IL\text{-}33}$ cultures were incubated with C3H.SW GFP–MLL-AF9 leukemic cells at different ratios. After 6 h, cells were washed, stained with viability dye, and analyzed by flow cytometry. Human T9 or $T9_{IL\text{-}33}$ were labeled with 5 µM CFSE and coincubated with MOLM14 leukemic cells labeled with 0.5 µM CFSE (Life Technologies). After 6 h, cells were washed and analyzed by flow cytometry. For imaging, cells were labeled with CD8α, CD8β, and SYTOX (S11348; ThermoFisher; SYTOX was added 5 min before acquisition). Images were acquired using Image Stream (Amnis) after 3 h of coincubation.

Colonic epithelial cell apoptosis assay

A BALB/c primary colonic epithelial cell line (BALB-5047; Cell Biological) was co-cultured together or separately (through a Transwell) with in vitro differentiated T9, WT $T9_{IL\text{-}33}$, or $ST2^{-/-}$ $T9_{IL\text{-}33}$ cells at a ratio of 1:10 with anti-AREG or the appropriate isotype control. 6 h later, cells were washed, stained with viability dye and Annexin V, and analyzed by flow cytometry. In some experiments, colonic epithelial cells were co-cultured with T1 + $T9_{IL\text{-}33}$ cells or T1 cells + in vitro polarized T reg cells purified magnetically using the $CD4^+CD25^+$ regulatory T cell isolation kit from Miltenyi (130-091-041) at a ratio of 1:1.

Human T1, T9, or $T9_{IL\text{-}33}$ cells were co-cultured with the primary colonic epithelial cell line (HNNC) in the presence of anti–human AREG or isotype control in the same conditions described above.

In vivo treatment with anti-AREG

C3H.SW recipients received 1,100 cGy total body irradiation (^{137}Cs source) on day −1. On day 0, mice were injected intravenously with B6 TCD BM cells (5×10^6) plus 3×10^6 in vitro differentiated WT $T9_{IL\text{-}33}$, cells. Mice received five doses of 100 µg anti-AREG or isotype control every other day from day −1 to day 7.

CD8α blocking

Anti-CD8α blocking antibody for mouse (53–6.7) or human (LT8) was added (both at 50 µg/ml) during differentiation of $T9_{IL\text{-}33}$ cells or during coincubation with MLL-AF9 leukemic cells.

Flow cytometry

All antibodies (Table S1) and reagents for flow cytometry were purchased from eBioscience, unless otherwise stated. The cells were preincubated with purified anti–mouse CD16/CD32 mAb for 15 min at 4°C to prevent nonspecific binding of the antibodies. The cells were subsequently incubated for 30 min at 4°C with antibodies for surface staining. Fixable viability dye was used to distinguish live cells from dead cells. The FoxP3/transcription factor staining buffer set and fixation and permeabilization kit were used for intracellular staining. For cytokine staining, cells were restimulated with 10 µg/ml anti-CD3 for 4–6 h, and brefeldin A was added for the last 2 h of culture.

MLR

Purified splenic total T cells from B6 WT, $ST2^{-/-}$, or $CD8\alpha^{-/-}$ mice were cultured with allogenic TCD and irradiated splenocytes (3,000 cGy) from BALB/c or C3H.SW mice in the presence of T1 or $T9_{IL\text{-}33}$ polarizing cytokines. On day 3, cells were expanded with fresh growth media in the presence of additional cytokines at the same concentrations as in day 0 medium. Splenic T cells from BALB/c or C3H.SW mice cultured under the same conditions were used as syngeneic controls.

Isolation of intestinal cells

Single-cell suspensions were prepared from intestines as described previously (Zhang et al., 2015). In brief, intestines were flushed with PBS to remove fecal matter and mucus. Fragments (<0.5 cm) of intestines were digested in 10 ml DMEM containing 2 mg/ml collagenase type B (Roche), 10 µg/ml deoxyribonuclease I (Roche), and 4% bovine serum albumin (Sigma-Aldrich) at 37°C with shaking for 90 min. The digested mixture was then diluted with 30 ml of plain DMEM, filtered through a 70-µm strainer, and centrifuged at 850 *g* for 10 min. The cell pellets were suspended in 5 ml of 80% Percoll (GE Healthcare), overlaid with 8 ml 40% Percoll, and spun at 2,000 rpm for 20 min at 4°C without braking. Enriched lymphocytes were collected from the interface. For sorting of intestinal stem cells, we did not perform Percoll separation.

Cell sorting

$CD4^+$ or $CD8^+$ T cells were harvested from in vitro differentiated WT $T9_{IL\text{-}33}$ or $ST2^{-/-}$ $T9_{IL\text{-}33}$ cells for quantitative RT-PCR and NanoString analysis. $CD4^+$ T cells and $CD8^+$ T cells were sorted from single-cell suspensions of intestine from GVHD mice at day 14 after transplantation of allogeneic T1, WT $T9_{IL\text{-}33}$, or $ST2^{-/-}$ $T9_{IL\text{-}33}$ cells. Cell sorting was performed using a BD FACSAria (BD Bioscience).

ACT of Foxp3-GFP $T9_{IL\text{-}33}$ cells

Total splenic T cells from B6 Foxp3-GFP reporter mice were purified via magnetic bead selection (Miltenyi Biotec). Cells were plated at a concentration of 1×10^6 cells/ml and activated with 1 μg/ml plate-bound anti-CD3 (2C11) and 5–10 μg/ml soluble anti-CD28 (37.51). $CD4^+$ and $CD8^+$ cells were polarized toward $T9_{IL33}$ cells as described before. 5 d later, cells were harvested and sorted to obtain Foxp3-GFP cells. Then, 3×10^6 Foxp3-GFP–depleted or nondepleted cells were injected with 5×10^6 TCD BM cells into lethally irradiated C3H.SW mice.

Histopathological analysis of GVHD

Specimens of liver and intestine were made of formalin-preserved tissue by the Pathology Department at Indiana University Medical Center. The slides were coded without reference to previous treatment and examined in a blinded fashion by C. Liu (Rutgers Robert Wood Johnson Medical School, New Brunswick, NJ). A semiquantitative scoring system was used to assess abnormalities known to be associated with GVHD. After scoring, the codes were broken and the data were compiled.

T reg isolation

T reg cells were isolated magnetically from fresh splenocytes or in vitro polarized toward T reg cells (10 ng/ml IL-2 and 10 ng/ml TGF-β) using the $CD4^+CD25^+$ regulatory T cell isolation kit.

Quantitative RT-PCR

Total RNA was isolated from sorted cells using the RNeasy Plus Mini kit (QIAGEN). cDNA was prepared with SuperScript VILO cDNA Synthesis kit (Invitrogen). Quantitative RT-PCR was performed using SYBR green PCR mix on an ABI Prism 7500HT (Applied Biosystems). Thermocycler conditions included a 2-min incubation at 50°C and then 95°C for 10 min, followed by a two-step PCR program of 95°C for 5 s and 60°C for 60 s for 40 cycles. β-Actin was used as an internal control. The primer sequences were as follows: actin forward: 5′-CTCTGGCTCCTAGCACCATGAAGA-3′, reverse: 5′-GTAAAACGCAGCTCAGTAACAGTCCG-3′; ST2L forward: 5′-AAGGCACACCATAAGGCTGA-3′; reverse: 5′-TCGTAGAGCTTGCCATCGTT-3′; IL-9r forward: 5′-CACAAATGCACCTTCTGGGACA-3′, reverse: 5′-TCACTCCAACGATACGGTCCTT-3′; AREG forward: 5′-GGACAATGCAGGGTAAAAGTTGA-3′, reverse: 5′-TGAAAGAAGGACCAATGTCATTTC-3′; EGFR forward: 5′-TTGGCCTATTCATGCGAAGAC-3′, reverse: 5′-GAGGTTCCACGAGCTCTCTCTCT-3′.

Nanostring

Sorted $CD4^+$ or $CD8^+$ T cells from WT or $ST2^{-/-}$ $T9_{IL\text{-}33}$ cells were prepared for NanoString analysis as described previously (Zhang et al., 2015). In brief, RNA was isolated from sorted cells using the RNeasy Plus Mini kit (QIAGEN). NanoString analysis was performed with the nCounter Analysis System at NanoString Technologies. The nCounter Mouse Immunology kit, which includes 561 immunology-related mouse genes, was used.

ELISA

Concentrations of IFN-γ, TNF, IL-9, and IL-4 in the culture supernatant or plasma were measured with the DuoSet ELISA kits; sST2 was measured with the Quantikine ELISA kit (R&D Systems).

Statistical analysis

A log-rank test was used for survival analysis. Differences between two groups were compared using two-tailed unpaired *t* tests using GraphPad Prism software (version 6.05). Data in graphs represent mean ± SEM. P-values less than 0.05 were considered significant.

Online supplemental material

Fig. S1 shows that no expansion of T reg cells occurred during murine $T9_{IL\text{-}33}$ differentiation in vitro. Fig. S2 shows the total number of transcripts reads in the transcriptome analysis for *Gzma*, *Gzmb*, *Prf1*, *Fas*, *Cd27*, *Cd62l*, and *Cd8a* in sorted WT $T9_{IL\text{-}33}$ versus $ST2^{-/-}$ $T9_{IL\text{-}33}$ CD8 and CD4. Table S1 lists all antibodies used for the flow cytometry analyses. Table S2, included in a separate PDF, provides the raw data of the transcriptome analysis on sorted CD8 and CD4 cells from WT $T9_{IL\text{-}33}$ versus $ST2^{-/-}$ $T9_{IL\text{-}33}$ cells.

ACKNOWLEDGMENTS

The authors thank Drs. McKenzie and Rosenkranz for providing the $ST2^{-/-}$ and $IL\text{-}9^{-/-}$ mice.

The authors are supported by the National Cancer Institute (grant R01CA168814), the Leukemia and Lymphoma Society (grant 1293-15), and the Lilly Physician Scientist Initiative Award.

S. Paczesny has a patent on "Methods of detection of graft-versus-host disease" licensed to Viracor-IBT Laboratories. The remaining authors declare no competing financial interests.

Author contributions: A. Ramadan designed and performed research, analyzed data, and wrote the paper. B. Griesenauer and D. Adom performed research, analyzed data, and wrote the paper. C. Liu graded and scored GVHD histopathology. R. Kapur, H. Hanenberg, and M.H. Kaplan provided essential materials and provided intellectual input; S. Paczesny conceived the project, designed experiments, analyzed data, and wrote the paper.

Submitted: 7 January 2017
Revised: 31 July 2017
Accepted: 8 September 2017

REFERENCES

American Cancer Society. 2015. Cancer Facts & Figures 2015. American Cancer Society, Atlanta. https://www.cancer.org/research/cancer-facts-statistics/all-cancer-facts-figures/cancer-facts-figures-2015.html.

Arpaia, N., J.A. Green, B. Moltedo, A. Arvey, S. Hemmers, S. Yuan, P.M. Treuting, and A.Y. Rudensky. 2015. A Distinct Function of Regulatory T Cells in Tissue Protection. *Cell*. 162:1078–1089. https://doi.org/10.1016/j.cell.2015.08.021

Baba, Y., K. Maeda, T. Yashiro, E. Inage, F. Niyonsaba, M. Hara, R. Suzuki, Y. Ohtsuka, T. Shimizu, H. Ogawa, et al. 2012. Involvement of PU.1 in mast cell/basophil-specific function of the human IL1RL1/ST2 promoter. *Allergol. Int.* 61:461–467. https://doi.org/10.2332/allergolint.12-OA-0424

Bachireddy, P., U.E. Burkhardt, M. Rajasagi, and C.J. Wu. 2015. Haematological malignancies: at the forefront of immunotherapeutic innovation. *Nat. Rev. Cancer.* 15:201–215. https://doi.org/10.1038/nrc3907

Badovinac, V.P., A.R. Tvinnereim, and J.T. Harty. 2000. Regulation of antigen-specific CD8+ T cell homeostasis by perforin and interferon-gamma. *Science.* 290:1354–1358. https://doi.org/10.1126/science.290.5495.1354

Blom, L., B.C. Poulsen, B.M. Jensen, A. Hansen, and L.K. Poulsen. 2011. IL-33 induces IL-9 production in human CD4+ T cells and basophils. *PLoS One.* 6:e21695. https://doi.org/10.1371/journal.pone.0021695

Bonilla, W.V., A. Fröhlich, K. Senn, S. Kallert, M. Fernandez, S. Johnson, M. Kreutzfeldt, A.N. Hegazy, C. Schrick, P.G. Fallon, et al. 2012. The alarmin interleukin-33 drives protective antiviral $CD8^+$ T cell responses. *Science.* 335:984–989. https://doi.org/10.1126/science.1215418

Chang, H.C., S. Zhang, V.T. Thieu, R.B. Slee, H.A. Bruns, R.N. Laribee, M.J. Klemsz, and M.H. Kaplan. 2005. PU.1 expression delineates heterogeneity in primary Th2 cells. *Immunity.* 22:693–703. https://doi.org/10.1016/j.immuni.2005.03.016

Chang, H.C., S. Sehra, R. Goswami, W. Yao, Q. Yu, G.L. Stritesky, R. Jabeen, C. McKinley, A.N. Ahyi, L. Han, et al. 2010. The transcription factor PU.1 is required for the development of IL-9-producing T cells and allergic inflammation. *Nat. Immunol.* 11:527–534. https://doi.org/10.1038/ni.1867

Cooke, K.R., L. Kobzik, T.R. Martin, J. Brewer, J. Delmonte Jr., J.M. Crawford, and J.L. Ferrara. 1996. An experimental model of idiopathic pneumonia syndrome after bone marrow transplantation: I. The roles of minor H antigens and endotoxin. *Blood.* 88:3230–3239.

Crespo, J., H. Sun, T.H. Welling, Z. Tian, and W. Zou. 2013. T cell anergy, exhaustion, senescence, and stemness in the tumor microenvironment. *Curr. Opin. Immunol.* 25:214–221. https://doi.org/10.1016/j.coi.2012.12.003

Cruz, C.R., and C.M. Bollard. 2015. T-cell and natural killer cell therapies for hematologic malignancies after hematopoietic stem cell transplantation: enhancing the graft-versus-leukemia effect. *Haematologica.* 100:709–719. https://doi.org/10.3324/haematol.2014.113860

Dardalhon, V., A. Awasthi, H. Kwon, G. Galileos, W. Gao, R.A. Sobel, M. Mitsdoerffer, T.B. Strom, W. Elyaman, I.C. Ho, et al. 2008. IL-4 inhibits TGF-beta-induced Foxp3+ T cells and, together with TGF-beta, generates IL-9+ IL-10+ Foxp3(-) effector T cells. *Nat. Immunol.* 9:1347–1355. https://doi.org/10.1038/ni.1677

de la Calle-Martin, O., M. Hernandez, J. Ordi, N. Casamitjana, J.I. Arostegui, I. Caragol, M. Ferrando, M. Labrador, J.L. Rodriguez-Sanchez, and T. Espanol. 2001. Familial CD8 deficiency due to a mutation in the CD8 alpha gene. *J. Clin. Invest.* 108:117–123. https://doi.org/10.1172/JCI10993

Dotti, G. 2015. Control of leukemia relapse after allogeneic hematopoietic stem cell transplantation: integrating transplantation with genetically modified T cell therapies. *Curr. Opin. Hematol.* 22:489–496. https://doi.org/10.1097/MOH.0000000000000177

Dunn, G.P., C.M. Koebel, and R.D. Schreiber. 2006. Interferons, immunity and cancer immunoediting. *Nat. Rev. Immunol.* 6:836–848. https://doi.org/10.1038/nri1961

Fontenot, J.D., M.A. Gavin, and A.Y. Rudensky. 2003. Foxp3 programs the development and function of CD4+CD25+ regulatory T cells. *Nat. Immunol.* 4:330–336. https://doi.org/10.1038/ni904

Fowler, D.H., J. Odom, S.M. Steinberg, C.K. Chow, J. Foley, Y. Kogan, J. Hou, J. Gea-Banacloche, C. Sportes, S. Pavletic, et al. 2006. Phase I clinical trial of costimulated, IL-4 polarized donor CD4+ T cells as augmentation of allogeneic hematopoietic cell transplantation. *Biol. Blood Marrow Transplant.* 12:1150–1160. https://doi.org/10.1016/j.bbmt.2006.06.015

Fung-Leung, W.P., M.W. Schilham, A. Rahemtulla, T.M. Kündig, M. Vollenweider, J. Potter, W. van Ewijk, and T.W. Mak. 1991. CD8 is needed for development of cytotoxic T cells but not helper T cells. *Cell.* 65:443–449. https://doi.org/10.1016/0092-8674(91)90462-8

Ghosh, S., M. Sarkar, T. Ghosh, I. Guha, A. Bhuniya, J. Biswas, A. Mallick, A. Bose, and R. Baral. 2016. Absence of CD4(+) T cell help generates corrupt CD8(+) effector T cells in sarcoma-bearing Swiss mice treated with NLGP vaccine. *Immunol. Lett.* 175:31–39. https://doi.org/10.1016/j.imlet.2016.05.004

Grupp, S.A., M. Kalos, D. Barrett, R. Aplenc, D.L. Porter, S.R. Rheingold, D.T. Teachey, A. Chew, B. Hauck, J.F. Wright, et al. 2013. Chimeric antigen receptor-modified T cells for acute lymphoid leukemia. *N. Engl. J. Med.* 368:1509–1518. https://doi.org/10.1056/NEJMoa1215134

Huang, Y., F. Clarke, M. Karimi, N.H. Roy, E.K. Williamson, M. Okumura, K. Mochizuki, E.J. Chen, T.J. Park, G.F. Debes, et al. 2015. CRK proteins selectively regulate T cell migration into inflamed tissues. *J. Clin. Invest.* 125:1019–1032. https://doi.org/10.1172/JCI77278

Jabeen, R., R. Goswami, O. Awe, A. Kulkarni, E.T. Nguyen, A. Attenasio, D. Walsh, M.R. Olson, M.H. Kim, R.S. Tepper, et al. 2013. Th9 cell development requires a BATF-regulated transcriptional network. *J. Clin. Invest.* 123:4641–4653. https://doi.org/10.1172/JCI69489

Joshi, N.S., W. Cui, A. Chandele, H.K. Lee, D.R. Urso, J. Hagman, L. Gapin, and S.M. Kaech. 2007. Inflammation directs memory precursor and short-lived effector CD8(+) T cell fates via the graded expression of T-bet transcription factor. *Immunity.* 27:281–295. https://doi.org/10.1016/j.immuni.2007.07.010

Jung, A.C., S. Guihard, S. Krugell, S. Ledrappier, A. Brochot, V. Dalstein, S. Job, A. de Reynies, G. Noël, B. Wasylyk, et al. 2013. CD8-alpha T-cell infiltration in human papillomavirus-related oropharyngeal carcinoma correlates with improved patient prognosis. *Int. J. Cancer.* 132:E26–E36. https://doi.org/10.1002/ijc.27776

Jung, U., J.E. Foley, A.A. Erdmann, M.A. Eckhaus, and D.H. Fowler. 2003. CD3/CD28-costimulated T1 and T2 subsets: differential in vivo allosensitization generates distinct GVT and GVHD effects. *Blood.* 102:3439–3446. https://doi.org/10.1182/blood-2002-12-3936

Kang, Y.J., X. Wang, S.J. Lin, Y.M. Hsu, and H.C. Chang. 2010. An active CD8alpha/pMHCI interaction is required for CD8 single positive thymocyte differentiation. *Eur. J. Immunol.* 40:836–848. https://doi.org/10.1002/eji.200939663

Kaplan, M.H., M.M. Hufford, and M.R. Olson. 2015. The development and in vivo function of T helper 9 cells. *Nat. Rev. Immunol.* 15:295–307. https://doi.org/10.1038/nri3824

Kenderian, S.S., M. Ruella, O. Shestova, M. Klichinsky, V. Aikawa, J.J. Morrissette, J. Scholler, D. Song, D.L. Porter, M. Carroll, et al. 2015. CD33-specific chimeric antigen receptor T cells exhibit potent preclinical activity against human acute myeloid leukemia. *Leukemia.* 29:1637–1647. https://doi.org/10.1038/leu.2015.52

Kim, I.K., B.S. Kim, C.H. Koh, J.W. Seok, J.S. Park, K.S. Shin, E.A. Bae, G.E. Lee, H. Jeon, J. Cho, et al. 2015. Glucocorticoid-induced tumor necrosis factor receptor-related protein co-stimulation facilitates tumor regression by inducing IL-9-producing helper T cells. *Nat. Med.* 21:1010–1017. https://doi.org/10.1038/nm.3922

Klebanoff, C.A., L. Gattinoni, P. Torabi-Parizi, K. Kerstann, A.R. Cardones, S.E. Finkelstein, D.C. Palmer, P.A. Antony, S.T. Hwang, S.A. Rosenberg, et al. 2005. Central memory self/tumor-reactive CD8+ T cells confer superior antitumor immunity compared with effector memory T cells. *Proc. Natl. Acad. Sci. USA.* 102:9571–9576. https://doi.org/10.1073/pnas.0503726102

Klebanoff, C.A., C.D. Scott, A.J. Leonardi, T.N. Yamamoto, A.C. Cruz, C. Ouyang, M. Ramaswamy, R. Roychoudhuri, Y. Ji, R.L. Eil, et al. 2016. Memory T cell-driven differentiation of naive cells impairs adoptive immunotherapy. *J. Clin. Invest.* 126:318–334. https://doi.org/10.1172/JCI81217

Koch, S., A. Larbi, E. Derhovanessian, D. Ozcelik, E. Naumova, and G. Pawelec. 2008. Multiparameter flow cytometric analysis of CD4 and CD8 T cell subsets in young and old people. *Immun. Ageing.* 5:6. https://doi.org/10.1186/1742-4933-5-6

Löhning, M., A. Stroehmann, A.J. Coyle, J.L. Grogan, S. Lin, J.C. Gutierrez-Ramos, D. Levinson, A. Radbruch, and T. Kamradt. 1998. T1/ST2 is preferentially expressed on murine Th2 cells, independent of interleukin 4, interleukin 5, and interleukin 10, and important for Th2 effector function. *Proc. Natl. Acad. Sci. USA.* 95:6930–6935. https://doi.org/10.1073/pnas.95.12.6930

Lu, Y., S. Hong, H. Li, J. Park, B. Hong, L. Wang, Y. Zheng, Z. Liu, J. Xu, J. He, et al. 2012. Th9 cells promote antitumor immune responses in vivo. *J. Clin. Invest.* 122:4160–4171. https://doi.org/10.1172/JCI65459

Lu, Y., B. Hong, H. Li, Y. Zheng, M. Zhang, S. Wang, J. Qian, and Q. Yi. 2014. Tumor-specific IL-9-producing CD8+ Tc9 cells are superior effector than type-I cytotoxic Tc1 cells for adoptive immunotherapy of cancers. *Proc. Natl. Acad. Sci. USA.* 111:2265–2270. https://doi.org/10.1073/pnas.1317431111

Mangus, C.W., P.R. Massey, D.H. Fowler, and S. Amarnath. 2013. Rapamycin resistant murine th9 cells have a stable in vivo phenotype and inhibit graft-versus-host reactivity. *PLoS One.* 8:e72305. https://doi.org/10.1371/journal.pone.0072305

Matta, B.M., D.K. Reichenbach, X. Zhang, L. Mathews, B.H. Koehn, G.K. Dwyer, J.M. Lott, F.M. Uhl, D. Pfeifer, C.J. Feser, et al. 2016. Peri-alloHCT IL-33 administration expands recipient T-regulatory cells that protect mice against acute GVHD. *Blood.* 128:427–439. https://doi.org/10.1182/blood-2015-12-684142

Monticelli, L.A., L.C. Osborne, M. Noti, S.V. Tran, D.M. Zaiss, and D. Artis. 2015. IL-33 promotes an innate immune pathway of intestinal tissue protection dependent on amphiregulin-EGFR interactions. *Proc. Natl. Acad. Sci. USA.* 112:10762–10767. https://doi.org/10.1073/pnas.1509070112

Munneke, J.M., A.T. Björklund, J.M. Mjösberg, K. Garming-Legert, J.H. Bernink, B. Blom, C. Huisman, M.H. van Oers, H. Spits, K.J. Malmberg, and M.D. Hazenberg. 2014. Activated innate lymphoid cells are associated with a reduced susceptibility to graft-versus-host disease. *Blood.* 124:812–821. https://doi.org/10.1182/blood-2013-11-536888

Murakami-Satsutani, N., T. Ito, T. Nakanishi, N. Inagaki, A. Tanaka, P.T. Vien, K. Kibata, M. Inaba, and S. Nomura. 2014. IL-33 promotes the induction and maintenance of Th2 immune responses by enhancing the function of OX40 ligand. *Allergol. Int.* 63:443–455. https://doi.org/10.2332/allergolint.13-OA-0672

Olson, M.R., F.F. Verdan, M.M. Hufford, A.L. Dent, and M.H. Kaplan. 2016. STAT3 Impairs STAT5 Activation in the Development of IL-9-Secreting T Cells. *J. Immunol.* 196:3297–3304. https://doi.org/10.4049/jimmunol.1501801

Othus, M., F.R. Appelbaum, S.H. Petersdorf, K.J. Kopecky, M. Slovak, T. Nevill, J. Brandwein, R.A. Larson, P.J. Stiff, R.B. Walter, et al. 2015. Fate of patients with newly diagnosed acute myeloid leukemia who fail primary induction therapy. *Biol. Blood Marrow Transplant.* 21:559–564. https://doi.org/10.1016/j.bbmt.2014.10.025

Porter, D.L., W.T. Hwang, N.V. Frey, S.F. Lacey, P.A. Shaw, A.W. Loren, A. Bagg, K.T. Marcucci, A. Shen, V. Gonzalez, et al. 2015. Chimeric antigen receptor T cells persist and induce sustained remissions in relapsed refractory chronic lymphocytic leukemia. *Sci. Transl. Med.* 7:303ra139. https://doi.org/10.1126/scitranslmed.aac5415

Purwar, R., C. Schlapbach, S. Xiao, H.S. Kang, W. Elyaman, X. Jiang, A.M. Jetten, S.J. Khoury, R.C. Fuhlbrigge, V.K. Kuchroo, et al. 2012. Robust tumor immunity to melanoma mediated by interleukin-9-producing T cells. *Nat. Med.* 18:1248–1253. https://doi.org/10.1038/nm.2856

Reshef, R., S.M. Luger, E.O. Hexner, A.W. Loren, N.V. Frey, S.D. Nasta, S.C. Goldstein, E.A. Stadtmauer, J. Smith, S. Bailey, et al. 2012. Blockade of lymphocyte chemotaxis in visceral graft-versus-host disease. *N. Engl. J. Med.* 367:135–145. https://doi.org/10.1056/NEJMoa1201248

Riddle, D.S., P.J. Miller, B.G. Vincent, T.B. Kepler, R. Maile, J.A. Frelinger, and E.J. Collins. 2008. Rescue of cytotoxic function in the CD8alpha knockout mouse by removal of MHC class II. *Eur. J. Immunol.* 38:1511–1521. https://doi.org/10.1002/eji.200737710

Sallusto, F., D. Lenig, R. Förster, M. Lipp, and A. Lanzavecchia. 1999. Two subsets of memory T lymphocytes with distinct homing potentials and effector functions. *Nature.* 401:708–712. https://doi.org/10.1038/44385

Schiering, C., T. Krausgruber, A. Chomka, A. Fröhlich, K. Adelmann, E.A. Wohlfert, J. Pott, T. Griseri, J. Bollrath, A.N. Hegazy, et al. 2014. The alarmin IL-33 promotes regulatory T-cell function in the intestine. *Nature.* 513:564–568. https://doi.org/10.1038/nature13577

Song, A., J. Song, X. Tang, and M. Croft. 2007. Cooperation between CD4 and CD8 T cells for anti-tumor activity is enhanced by OX40 signals. *Eur. J. Immunol.* 37:1224–1232. https://doi.org/10.1002/eji.200636957

Staudt, V., E. Bothur, M. Klein, K. Lingnau, S. Reuter, N. Grebe, B. Gerlitzki, M. Hoffmann, A. Ulges, C. Taube, et al. 2010. Interferon-regulatory factor 4 is essential for the developmental program of T helper 9 cells. *Immunity.* 33:192–202. https://doi.org/10.1016/j.immuni.2010.07.014

Tamiya, T., K. Ichiyama, H. Kotani, T. Fukaya, T. Sekiya, T. Shichita, K. Honma, K. Yui, T. Matsuyama, T. Nakao, et al. 2013. Smad2/3 and IRF4 play a cooperative role in IL-9-producing T cell induction. *J. Immunol.* 191:2360–2371. https://doi.org/10.4049/jimmunol.1301276

Tawara, I., Y. Maeda, Y. Sun, K.P. Lowler, C. Liu, T. Toubai, A.N. McKenzie, and P. Reddy. 2008. Combined Th2 cytokine deficiency in donor T cells aggravates experimental acute graft-vs-host disease. *Exp. Hematol.* 36:988–996. https://doi.org/10.1016/j.exphem.2008.02.010

van den Brink, M.R., and S.J. Burakoff. 2002. Cytolytic pathways in haematopoietic stem-cell transplantation. *Nat. Rev. Immunol.* 2:273–281. https://doi.org/10.1038/nri775

Vander Lugt, M.T., T.M. Braun, S. Hanash, J. Ritz, V.T. Ho, J.H. Antin, Q. Zhang, C.H. Wong, H. Wang, A. Chin, et al. 2013. ST2 as a marker for risk of therapy-resistant graft-versus-host disease and death. *N. Engl. J. Med.* 369:529–539. https://doi.org/10.1056/NEJMoa1213299

Vasanthakumar, A., K. Moro, A. Xin, Y. Liao, R. Gloury, S. Kawamoto, S. Fagarasan, L.A. Mielke, S. Afshar-Sterle, S.L. Masters, et al. 2015. The transcriptional regulators IRF4, BATF and IL-33 orchestrate development and maintenance of adipose tissue-resident regulatory T cells. *Nat. Immunol.* 16:276–285. https://doi.org/10.1038/ni.3085

Végran, F., H. Berger, R. Boidot, G. Mignot, M. Bruchard, M. Dosset, F. Chalmin, C. Rébé, V. Dérangère, B. Ryffel, et al. 2014. The transcription factor IRF1 dictates the IL-21-dependent anticancer functions of TH9 cells. *Nat. Immunol.* 15:758–766. https://doi.org/10.1038/ni.2925

Veldhoen, M., C. Uyttenhove, J. van Snick, H. Helmby, A. Westendorf, J. Buer, B. Martin, C. Wilhelm, and B. Stockinger. 2008. Transforming growth factor-beta 'reprograms' the differentiation of T helper 2 cells and promotes an interleukin 9-producing subset. *Nat. Immunol.* 9:1341–1346. https://doi.org/10.1038/ni.1659

Waldman, E., S.X. Lu, V.M. Hubbard, A.A. Kochman, J.M. Eng, T.H. Terwey, S.J. Muriglan, T.D. Kim, G. Heller, G.F. Murphy, et al. 2006. Absence of beta7 integrin results in less graft-versus-host disease because of decreased homing of alloreactive T cells to intestine. *Blood*. 107:1703–1711. https://doi.org/10.1182/blood-2005-08-3445

Wang, Y., Y. Bi, X. Chen, C. Li, Y. Li, Z. Zhang, J. Wang, Y. Lu, Q. Yu, H. Su, et al. 2016. Histone deacetylase SIRT1 negatively regulates the differentiation of interleukin-9-producing CD4(+) T cells. *Immunity.* 44:1337–1349. https://doi.org/10.1016/j.immuni.2016.05.009

Warren, E.H., and H.J. Deeg. 2013. Dissecting graft-versus-leukemia from graft-versus-host-disease using novel strategies. *Tissue Antigens*. 81:183–193. https://doi.org/10.1111/tan.12090

Xiao, X., S. Balasubramanian, W. Liu, X. Chu, H. Wang, E.J. Taparowsky, Y.X. Fu, Y. Choi, M.C. Walsh, and X.C. Li. 2012. OX40 signaling favors the induction of T(H)9 cells and airway inflammation. *Nat. Immunol.* 13:981–990. https://doi.org/10.1038/ni.2390

Xu, D., W.L. Chan, B.P. Leung, F. Huang, R. Wheeler, D. Piedrafita, J.H. Robinson, and F.Y. Liew. 1998. Selective expression of a stable cell surface molecule on type 2 but not type 1 helper T cells. *J. Exp. Med.* 187:787–794. https://doi.org/10.1084/jem.187.5.787

Zaiss, D.M., J. van Loosdregt, A. Gorlani, C.P. Bekker, A. Gröne, M. Sibilia, P.M. van Bergen en Henegouwen, R.C. Roovers, P.J. Coffer, and A.J. Sijts. 2013. Amphiregulin enhances regulatory T cell-suppressive function via the epidermal growth factor receptor. *Immunity.* 38:275–284. https://doi.org/10.1016/j.immuni.2012.09.023

Zhang, J., A.M. Ramadan, B. Griesenauer, W. Li, M.J. Turner, C. Liu, R. Kapur, H. Hanenberg, B.R. Blazar, I. Tawara, and S. Paczesny. 2015. ST2 blockade reduces sST2-producing T cells while maintaining protective mST2-expressing T cells during graft-versus-host disease. *Sci. Transl. Med.* 7:308ra160. https://doi.org/10.1126/scitranslmed.aab0166